

# Thermal Conductivity of $\text{MgO}$ , $\text{Al}_2\text{O}_3$ , $\text{MgAl}_2\text{O}_4$ , and $\text{Fe}_3\text{O}_4$ Crystals from 3° to 300°K\*

GLEN A. SLACK

General Electric Research Laboratory, Schenectady, New York

(Received October 31, 1961; revised manuscript received January 12, 1962)

The thermal conductivity from 3° to 300°K of single crystals of the two spinels, diamagnetic  $\text{MgAl}_2\text{O}_4$  and paramagnetic  $\text{Fe}_3\text{O}_4$ , has been measured and analyzed. The heat is transported by phonons in both cases. The phonon scattering processes in the two crystals are quite similar except that the phonons in  $\text{Fe}_3\text{O}_4$  are also scattered by the magnetic lattice in its disordered state. The thermal conductivity of  $\text{Fe}_3\text{O}_4$  falls abruptly with increasing temperature at the  $121 \pm 2^\circ\text{K}$  transition.

Comparison of results on the double oxide  $\text{MgAl}_2\text{O}_4$  with those on the single oxides  $\text{MgO}$  and  $\alpha\text{-Al}_2\text{O}_3$  indicates the double oxide has an intermediate thermal conductivity. Measurements on crystals of  $\text{MgO} \cdot 3.5\text{Al}_2\text{O}_3$  and  $\text{Mg}_x\text{Fe}_y\text{Al}_z\text{O}_4$  from 3° to 300°K indicate that vacancies and certain impurities can noticeably lower the thermal conductivity of  $\text{MgAl}_2\text{O}_4$ . The effect of vacancies and impurities on  $\text{Fe}_3\text{O}_4$  is also noticeable, particularly below 30°K.

## INTRODUCTION

THE thermal conductivity of transition metal compounds which are electrically nonconducting or are semiconducting has not been studied very extensively in the past. The main interest at present is to study compounds in which most if not all of the thermal energy is transported by phonons, and possibly by magnons. If the thermal conductivity is measured over a wide range of temperatures, particularly through regions of magnetic transitions, or phase transitions, it may be possible to gain some insight into the interaction of phonons with the magnetic moments in the solid.

In this paper a brief summary is given of the thermal conductivity measurements available in the literature for paramagnetic transition metal compounds of the first transition metal series in which anomalous behavior has been seen. A few cases can be found where a magnetic or crystallographic change is associated with a change in thermal conductivity. In the next section an understanding of the thermal conductivity as a function of temperature for pure and impure spinel,  $\text{MgAl}_2\text{O}_4$ , is developed by comparison of this double oxide with the single constituent oxides  $\text{MgO}$  and  $\alpha\text{-Al}_2\text{O}_3$ . Then these results on diamagnetic  $\text{MgAl}_2\text{O}_4$  are employed to help understand the thermal conductivity of  $\text{Fe}_3\text{O}_4$ , which has the same spinel crystal structure. The observation is that in  $\text{Fe}_3\text{O}_4$  and related ferrites there is an additional phonon scattering caused by interaction of the phonons with the magnetic moments.

## PREVIOUS WORK

The present measurements on  $\text{Fe}_3\text{O}_4$  single crystals provide a system in which the interaction of phonons and magnetic moments is particularly pronounced. Before considering these results it is instructive to consider the previous work that has been done on the thermal conductivity of some transition metal compounds. Probably some of the earliest such measure-

ments were reported in 1905 by Kruckenberg<sup>1</sup> on natural crystals of  $\text{Fe}_3\text{O}_4$  and  $\text{Fe}_2\text{O}_3$  at 343°K. In 1911 Koenigsberger and Weiss<sup>2</sup> also reported measurements on a natural crystal of  $\text{Fe}_2\text{O}_3$  at 303°K. Some average results on ceramic ferrites at 300°K have recently been reported by Smit and Wijn.<sup>3</sup>

None of these measurements have been made as a function of temperature, and it is the temperature dependence of the thermal conductivity that provides the most useful information about the phonon interactions. In 1917 Bidwell<sup>4</sup> reported what were probably the first measurements on a transition metal compound as a function of temperature. He studied a ceramic sample of  $\text{Fe}_2\text{O}_3$  from 430° to 1320°K. Even though his absolute values of the thermal conductivity  $K$  are unreasonably low, and his temperature dependence seems wrong for a low porosity sample, he does observe an inflection in the  $K$  versus  $T$  curve at 980°K. This is quite close to the reported<sup>5</sup> Curie temperature  $T_c$  for  $\alpha\text{-Fe}_2\text{O}_3$  at 950°K. It seems reasonable to attribute this inflection to the change in phonon scattering with temperature as the sample changes from the ferrimagnetic to the paramagnetic state. His measurements do not extend to temperatures low enough to cover the transition in  $\alpha\text{-Fe}_2\text{O}_3$  at 260°K.<sup>6</sup> Measurements of the  $K$  of single crystals of Mn and Co ferrite have recently been made between 1.5° and 25°K by Douthett and Friedberg.<sup>7</sup> In this temperature range none of the samples possess a magnetic or crystallographic transition, so that no anomalies in  $K$  versus  $T$  were observed. They did, however, observe a change in the phonon scattering as a function of applied magnetic field. Ceramic samples of NiO have been studied

<sup>1</sup> I. Kruckenberg, Arkiv Matematik, Astoromi, Fysik 2, 1 (1905).

<sup>2</sup> J. Koenigsberger and J. Weiss, Ann. Physik 35, 1 (1911).

<sup>3</sup> J. Smit and H. P. J. Wijn, *Advances in Electronics and Electron Physics*, edited by L. Marton (Academic Press Inc., New York, 1954), Vol. 6, pp. 69, 133; *Ferrites* (John Wiley & Sons, Inc., New York, 1959), p. 225.

<sup>4</sup> C. C. Bidwell, Phys. Rev. 10, 756 (1917).

<sup>5</sup> K. Endo, Sci. Repts. Tôhoku Univ. 25, 879 (1937).

<sup>6</sup> L. M. Corliss, J. M. Hastings, and J. E. Goldman, Phys. Rev. 93, 893 (1954).

<sup>7</sup> D. Douthett and S. A. Friedberg, Phys. Rev. 121, 1662 (1961).

\* This work was supported in part by the Wright Air Development Division, Ohio under Contract Number AF 33(616)-6499.

by Kingery *et al.*<sup>8</sup> from 420° to 1220°K. These measurements cover the  $T_N$  at 525°K,<sup>9</sup> but they show no anomaly to within the scatter of the data. Single crystals of MnO, and NiO have been measured by Slack and Newman,<sup>10</sup> and single crystals of CoO by Slack<sup>11</sup> from 3° to 300°K. Anomalies have been seen at the  $T_N$  values of 118°K for MnO,<sup>12</sup> and 290°K for CoO.<sup>13</sup> Anomalous behavior of the  $K$  of single crystals of MnF<sub>2</sub> and CoF<sub>2</sub>, measured from 3° to 300°K, has been observed by Slack<sup>14</sup> at their respective  $T_N$  values<sup>15</sup> of 67° and 38°K.

### PROCEDURE

There are two main problems. The first is to measure the thermal conductivity  $K$  of the diamagnetic spinel MgAl<sub>2</sub>O<sub>4</sub> versus temperature, and to explain its absolute magnitude and temperature dependence. Since MgAl<sub>2</sub>O<sub>4</sub> is a double oxide, the results can be compared with the  $K$  measurements on single crystal samples of the constituent oxides, MgO and  $\alpha$ -Al<sub>2</sub>O<sub>3</sub>. The question raised here is whether or not the double oxide has a  $K$  significantly different from that of the single constituent oxides.

MgAl<sub>2</sub>O<sub>4</sub> was chosen in order to have a comparison for Fe<sub>3</sub>O<sub>4</sub>. Actually there are a number of diamagnetic spinels to choose from. For example, MgAl<sub>2</sub>O<sub>4</sub> and ZnGa<sub>2</sub>O<sub>4</sub> both have the spinel structure, and the atomic weights of the two cations in each one are not very different ( $\leq 10\%$ ). MgAl<sub>2</sub>O<sub>4</sub> is a normal rather than inverse spinel<sup>16</sup> in that the Al<sup>3+</sup> ions are on the octahedral sites, and the Mg<sup>2+</sup> ions are on the tetrahedral ones. It is known<sup>17</sup> that CdGa<sub>2</sub>O<sub>4</sub> is a normal spinel, and from the calculations of Miller<sup>18</sup> it can be concluded that ZnGa<sub>2</sub>O<sub>4</sub> is also a normal spinel. However, the only single crystals that were available were those of MgAl<sub>2</sub>O<sub>4</sub>. Natural crystals of MgAl<sub>2</sub>O<sub>4</sub> are quite common,<sup>19</sup> and can be obtained through gem and jewelry sources in sizes large enough to enable useful measurements to be made. The technical problems of making large synthetic single crystals of MgAl<sub>2</sub>O<sub>4</sub> are quite

TABLE I. Description of the samples studied.<sup>a</sup>

Crystal	Run No.	$S$ (cm)	$d$ (cm)	$a_0$ (Å)
MgO	14	1.24	0.41	4.213 <sup>b</sup>
MgO	38	1.11	0.28	4.213 <sup>b</sup>
MgAl <sub>2</sub> O <sub>4</sub>	42	0.29	0.18	8.0866 <sup>c</sup>
MgAl <sub>2</sub> O <sub>4</sub>	54	0.45	0.25	8.0868 <sup>c</sup>
MgO·3.5Al <sub>2</sub> O <sub>3</sub>	53	1.12	0.40	7.979 <sup>c</sup>
Mg <sub>0.75</sub> Fe <sub>0.41</sub> Al <sub>1.85</sub> O <sub>4</sub>	56	1.12	0.34	8.128 <sup>c</sup>
Mg <sub>0.73</sub> Fe <sub>0.33</sub> Al <sub>1.93</sub> O <sub>4</sub>	62	1.00	0.24	8.117 <sup>c</sup>
Fe <sub>3</sub> O <sub>4</sub>	57	1.23	0.24	8.398 <sup>c</sup>
Fe <sub>3</sub> O <sub>4</sub>	37	1.26	0.54	8.397 <sup>c</sup>
Co <sub>0.07</sub> Fe <sub>2.93</sub> O <sub>4</sub>	63	0.80	0.24	8.394 <sup>c</sup>

<sup>a</sup>  $S$  = over-all length of the sample in the direction of heat flow.  $d$  = average diameter =  $(4A/\pi)^{1/2}$ , where  $A$  is the cross-sectional area perpendicular to the heat flow.  $a_0$  = lattice constant.

<sup>b</sup> See reference 32.

<sup>c</sup> Explicitly measured at 300°K for the samples as listed.

complex.<sup>20</sup> From the phase diagram studies<sup>21</sup> it appears to be easier to make nonstoichiometric Mg-Al spinels which are rich in Al<sub>2</sub>O<sub>3</sub>. Thus single crystals approximating the composition MgO·3.5 Al<sub>2</sub>O<sub>3</sub> are available commercially.<sup>22</sup> These nonstoichiometric Mg-Al spinels still possess the spinel crystal structure,<sup>20</sup> but the metal-ion-to-oxygen-ion ratio is less than 0.75. Hence there are vacancies in the metal ion lattice which noticeably affect the thermal conductivity.

Therefore, the natural, stoichiometric MgAl<sub>2</sub>O<sub>4</sub> crystals serve as the most useful comparison for Fe<sub>3</sub>O<sub>4</sub>. The nonstoichiometric, artificial Mg-Al-spinels provide us with information regarding the effect of large vacancy concentrations and partial inversion of the normal spinel structure on  $K$ .

The second problem is to explain the effect of phonon-magnetic moment interactions on the  $K$  of Fe<sub>3</sub>O<sub>4</sub> by using the results of MgAl<sub>2</sub>O<sub>4</sub> as a basis. Fe<sub>3</sub>O<sub>4</sub> magnetite, is ferrimagnetic, and is the starting point for many other ferrite materials.<sup>3</sup> It has a ferrimagnetic Curie temperature  $T_c$  of 848°K,<sup>23</sup> and an internal ordering transition at a transition temperature  $T_x$  of 119°K.<sup>24,25</sup> At all temperatures above  $T_x$ , samples of Fe<sub>3</sub>O<sub>4</sub> have the spinel crystal structure. In this structure there are both octahedral and tetrahedral sites for the metal ions, where there are 8×1 tetrahedral sites, 8×2 octahedral sites, and 8×4 oxygen sites in a unit cell of 8 molecules. In stoichiometric Fe<sub>3</sub>O<sub>4</sub> the tetrahedral sites are occupied by Fe<sup>3+</sup> ions, while half of the octahedral sites are occupied by the remaining Fe<sup>3+</sup> ions, and the other half by the Fe<sup>2+</sup> ions. Thus Fe<sub>3</sub>O<sub>4</sub> is an inverse spinel, as pointed out by Verwey and Haayman,<sup>26</sup> and con-

<sup>8</sup> W. D. Kingery, J. Francl, R. L. Coble, and T. Vasilos, J. Am. Ceram. Soc. **37**(II), 107 (1954).

<sup>9</sup> J. R. Tomlinson, L. Domash, R. C. Hay, and C. W. Montgomery, J. Am. Chem. Soc. **77**, 909 (1955).

<sup>10</sup> G. A. Slack and R. Newman, Phys. Rev. Letters **1**, 359 (1958).

<sup>11</sup> G. A. Slack, Bull. Am. Phys. Soc. **4**, 37 (1958); G. A. Slack, "Proceedings of the International Conference on Semiconductor Physics" (Czechoslovakia Academy of Science, Prague, 1961), p. 630.

<sup>12</sup> S. S. Todd and K. R. Bonnickson, J. Am. Chem. Soc. **73**, 3894 (1951).

<sup>13</sup> G. Assayag and H. Bizette, Compt. rend. **239**, 238 (1954).

<sup>14</sup> G. A. Slack, Phys. Rev. **122**, 1451 (1961).

<sup>15</sup> J. W. Stout and E. Catalano, J. Chem. Phys. **23**, 2013 (1955).

<sup>16</sup> G. E. Bacon, Acta Cryst. **5**, 684 (1952).

<sup>17</sup> W. Rudolf and B. Reuter, Z. anorg. u. allgem. Chem. **253**, 194 (1947).

<sup>18</sup> A. Miller, Suppl. J. Appl. Phys. **30**, 24S (1959).

<sup>19</sup> C. Palache, H. Berman, and C. Frondel, *Dana's System of Mineralogy* (John Wiley & Sons, Inc., New York, 1944), 7th ed., Vol. 1, p. 689.

<sup>20</sup> F. Rinne, Neues Jahrb. Mineral. Geol., beilage band **58A**, 43 (1928).

<sup>21</sup> D. M. Roy, R. Roy, and E. F. Osborn, Am. J. Sci. **251**, 337 (1953).

<sup>22</sup> Linde Air Products Company, New York, New York.

<sup>23</sup> D. O. Smith, Phys. Rev. **102**, 959 (1956).

<sup>24</sup> R. W. Millar, J. Am. Chem. Soc. **51**, 215 (1929).

<sup>25</sup> B. A. Calhoun, Phys. Rev. **94**, 1577 (1954).

<sup>26</sup> E. J. W. Verwey and P. W. Haayman, Physica **8**, 979 (1941).

TABLE II. Concentration of major impurities in the crystals by quantitative spectrographic analysis.

Crystal	MgO	MgO	MgAl <sub>2</sub> O <sub>4</sub>	MgAl <sub>2</sub> O <sub>4</sub>	MgO·3.5 Al <sub>2</sub> O <sub>3</sub>	Mg <sub>z</sub> Fe <sub>y</sub> Al <sub>x</sub> O <sub>4</sub>	Fe <sub>3</sub> O <sub>4</sub>
Run No.	14	38	42	54	53	56	37, 57
Impurity <sup>a</sup>							
Al	18.4	18.9	<i>m</i>	<i>m</i>	<i>m</i>	<i>m</i>	18.1
Be	18.4	18.4	<18.1	<18.1	<18.1	n.d.	<18.2
Ca	18.3	18.7	17.7	<17.7	17.4	n.d.	<17.9
Cr	17.6	17.6	19.2	19.3	<17.6	low	17.8
Fe	17.6	17.6	18.9	19.2	18.8	<i>m</i>	<i>m</i>
K	18.4	<18.4	17.7	18.3	<17.7	n.d.	<17.9
Li	17.5	17.5	18.2	18.2	18.0	n.d.	<18.1
Mg	<i>m</i>	<i>m</i>	<i>m</i>	<i>m</i>	<i>m</i>	<i>m</i>	17.6
Mn	<17.3	<17.3	18.1	17.9	<17.6	low	17.1
Na	18.7	18.7	18.3	18.3	18.0	n.d.	18.1
Ni	<17.2	<17.2	<17.6	<17.6	<17.6	low	17.6
Si	18.7	17.9	18.2	18.2	19.1	trace	<18.0
Ti	<17.6	<17.6	18.6	18.3	18.5	medium	<17.8
V	<17.3	<17.3	18.8	19.4	<17.6	low	<17.8
Zn	<17.8	<17.8	20.1	19.5	<17.8	low	<18.0
Zr	18.1	<17.7	<17.6	<17.4	<17.4	n.d.	<17.5

<sup>a</sup> The concentration of the *j*th type of impurity is  $\epsilon_{pj}$  in atoms/cm<sup>3</sup>. The entries in the table are  $\log_{10}\epsilon_{pj}$ . The letter *m* denotes a major constituent. Only qualitative values are given for the Mg<sub>z</sub>Fe<sub>y</sub>Al<sub>x</sub>O<sub>4</sub> spinel because it is very impure. Here n.d. = not detected. In these crystals, the total number of atoms/cm<sup>3</sup> is about  $1.0 \times 10^{23}$ . The metal impurities not listed may be present in concentrations less than  $10^{18}$  cm<sup>-3</sup>, except for R-56 for which this limit is about  $10^{19}$  cm<sup>-3</sup>.

firmed by the neutron scattering results of Shull, Wollan, and Koehler.<sup>27</sup>

#### SAMPLES

The single-crystal samples that were studied came from a variety of sources. The MgO, Fe<sub>3</sub>O<sub>4</sub>, and MgO·3.5 Al<sub>2</sub>O<sub>3</sub> were synthetic crystals. The MgAl<sub>2</sub>O<sub>4</sub> and Mg<sub>z</sub>Fe<sub>y</sub>Al<sub>x</sub>O<sub>4</sub> were natural crystals. These are listed in Table I. In addition, Table I contains the x-ray lattice constant at 300°K, the sample size, and the particular run number (e.g., R-) in which the thermal conductivity was measured.

The MgO crystals were supplied by Hansler,<sup>28</sup> and were grown from the melt in an arc furnace using carbon electrodes and a self-crucible technique.<sup>29</sup> They were transparent, colorless, well-formed, and free of visible defects. The Fe<sub>3</sub>O<sub>4</sub> crystals were grown by Horn<sup>30</sup> from the melt using the Czochralski technique. These were opaque, possessed a black luster, and contained no second phase inclusions of FeO or Fe<sub>2</sub>O<sub>3</sub>. The MgO·3.5 Al<sub>2</sub>O<sub>3</sub> crystals were obtained from Linde,<sup>22</sup> and were made by the Verneuil<sup>31</sup> process. These had the same outward appearance as the MgO crystals. Two different natural crystals of MgAl<sub>2</sub>O<sub>4</sub> both came from Burma. They were transparent and light pink in color, and were in the shape of small, imperfectly formed, single crystal octahedra before cutting to size.

The two Mg<sub>z</sub>Fe<sub>y</sub>Al<sub>x</sub>O<sub>4</sub> crystals were opaque, water worn, crystals of pleonaste spinel from Queensland, Australia. The chemical analyses indicated a formula of (Ti<sub>w</sub>Mg<sub>z</sub>Fe<sub>y</sub>Al<sub>x</sub>)O<sub>4</sub> for both crystals, where for R-56  $w=0.02$ ,  $x=0.75$ ,  $y=0.41$ ,  $z=1.85$ , and for R-62  $w=0.01$ ,  $x=0.73$ ,  $y=0.33$ ,  $z=1.93$ . Note that  $w+x+y+z=3.0$ . The Ti concentration in both is small enough to be neglected. Traces of other minor constituents are listed in Table II. Both pleonaste spinels were single crystals, as verified by x-ray studies, and were virtually free of second phase inclusions. Thin polished sections of the crystals 40  $\mu$  thick were transparent and yellow-brown in color. These sections indicated about 0.1% by volume of some unidentified second phase inclusions or pores.

The lattice constants of the natural MgAl<sub>2</sub>O<sub>4</sub> crystals are 0.08% larger than the value<sup>32</sup> of 8.0800 Å at 297°K for pure MgAl<sub>2</sub>O<sub>4</sub>. This discrepancy is probably not caused by a deviation from the stoichiometric MgO to Al<sub>2</sub>O<sub>3</sub> ratio of 1:1, but rather by the traces of other impurities which, from Table II, occupy about 0.2% of the metal ion lattice sites. The lattice constant of 7.979 Å for the synthetic spinel from Linde is considerably less than that for pure MgAl<sub>2</sub>O<sub>4</sub>. This difference is caused by the large excess of Al<sub>2</sub>O<sub>3</sub> compared to MgO. The Al<sub>2</sub>O<sub>3</sub> to MgO ratio was measured by chemical analysis for the present sample as  $3.7 \pm 0.3$ , and thus agrees with the manufacturers value of 3.5. Using the value of  $a_0=7.979$  Å and the variation of  $a_0$  of MgO-Al<sub>2</sub>O<sub>3</sub> solid solutions found by Roy, Roy, and Osborn<sup>31</sup> the computed Al<sub>2</sub>O<sub>3</sub> to MgO ratio is 3.3. This

<sup>27</sup> C. G. Shull, E. O. Wollan, and W. C. Koehler, Phys. Rev. 84, 912 (1951).

<sup>28</sup> R. L. Hansler, Lamp Division, General Electric Company, Cleveland, Ohio.

<sup>29</sup> H. Moissan, Ann. chim. et phys. 4, 136 (1895).

<sup>30</sup> F. H. Horn, J. Appl. Phys. 32, 900 (1961).

<sup>31</sup> A. Verneuil, Ann. chim. et phys. 3, 20 (1904).

<sup>32</sup> H. E. Swanson and E. Tagte, National Bureau of Standards Circular No. 539, 1953 (unpublished), Vol. 1, p. 38, 39.

is also in good agreement with the 3.5 value, which will be used hereafter.

The measured  $a_0$  of 8.398 Å for stoichiometric  $\text{Fe}_3\text{O}_4$  (R-57) agrees quite well with Hagg,<sup>33</sup> who found 8.397 Å, and with Abrahams and Calhoun,<sup>34</sup> who found 8.394 Å at 295°K. The iron deficiency in R-37 and the Co content of R-63 account for the slightly smaller  $a_0$  values. The lattice constant of the mixed Mg-Fe-Al spinels lie between the values for  $\text{MgAl}_2\text{O}_4$  and  $\text{FeAl}_2\text{O}_4$ , as might be expected. These limiting values<sup>35</sup> are  $a_0 = 8.135$  Å for  $\text{FeAl}_2\text{O}_4$  and 8.080 Å for  $\text{MgAl}_2\text{O}_4$ . These pleonaste spinels are essentially  $\text{MgAl}_2\text{O}_4$  with 25% of the  $\text{Mg}^{2+}$  and about 10% of the  $\text{Al}^{3+}$  replaced by  $\text{Fe}^{2+}$ . If the Ti is  $\text{Ti}^{4+}$ , the charge balance is maintained with practically all of the Fe in the  $\text{Fe}^{2+}$  state.

Since the effects of chemical impurities play a large part in determining thermal conductivity, a quantitative spectrochemical analysis was made for most of the samples. The impurity concentrations are given in Table II, and are probably accurate to within a factor of 2. For ease in tabulating, the  $\log_{10}$  of the impurity concentration is given. This method also allows a quick assessment of the order of magnitude of the impurity concentration. Note that all samples except  $\text{Fe}_3\text{O}_4$  have an aggregate impurity concentration of at least  $10^{19} \text{ cm}^{-3}$ , and some are much higher. In the  $\text{Fe}_3\text{O}_4$  the total concentration is  $4 \times 10^{18}$  and could probably be reduced to around  $10^{18} \text{ cm}^{-3}$  with improvements in the growing technique. These  $\text{Fe}_3\text{O}_4$  crystals were grown from iridium crucibles by the Czochralski technique,<sup>30</sup> the iridium content is less than  $3 \times 10^{17} \text{ cm}^{-3}$ . An analysis of R-63 is not given in Table II because it has the same purity as R-37 and R-57 except for the added cobalt.

In addition to foreign chemical impurities variable valence crystals like magnetite can possess large concentrations of vacancies. " $\text{Fe}_3\text{O}_4$ " can deviate substantially from an iron-to-oxygen ratio of exactly 3:4. For illustration, the fcc oxygen lattice and the spinel structure is maintained even for  $\gamma\text{-Fe}_2\text{O}_3$ . This crystal is essentially magnetite in which there are no  $\text{Fe}^{2+}$  ions,<sup>33,36</sup> and  $\frac{1}{6}$  of the octahedral lattice sites are vacant.<sup>37</sup> This corresponds to a fractional concentration of iron vacancies  $p$ , of  $\frac{1}{6}$ . That is, 11.1% of all the possible iron ion sites in the spinel lattice are unoccupied. Thus in magnetite crystals the limits on  $p$  are  $0 \leq p \leq 0.111$ . From the data of Greig *et al.*<sup>38</sup> and Darken and Gurry<sup>39</sup> the maximum value of  $p$  for magnetite at high temperatures in equilibrium under an oxygen partial pres-

sure  $P_{\text{O}_2}$  of 1 atmosphere is  $p = 0.034$  for a temperature of 1725°K. In an  $\text{O}_2/\text{CO}/\text{CO}_2$  environment at a total pressure of 1 atm produced by introducing pure  $\text{CO}_2$  at room temperature into the growing furnace, the maximum value is  $p = 0.010$  at 1375°K. The "as-grown" magnetite crystal measured in R-37 was analyzed by standard wet chemistry methods in order to determine the  $\text{Fe}^{2+}:\text{Fe}^{3+}$  ratio. The fractional vacancy concentration was  $p = 0.006$ , which corresponds to an equilibration temperature of about 1420°K in the  $\text{O}_2/\text{CO}/\text{CO}_2$  atmosphere of the growing furnace. This atmosphere corresponds to a partial pressure of oxygen of  $1 \times 10^{-4}$  atm. A section of the R-37 crystal, which is designated here as R-57, was subjected to an annealing of 1500°K in a  $\text{CO}/\text{CO}_2$  atmosphere with a ratio of 1 part CO to 20 parts  $\text{CO}_2$  by volume. This mixture produced an equilibrium partial pressure of oxygen of  $1 \times 10^{-8}$  atm at 1500°K. After this treatment the vacancy concentration is too low to measure by standard chemical techniques. However, an estimate of  $p$  can be made using the approach of Flood and Hill.<sup>40</sup> The value of  $p$ , computed from the data of Greig *et al.*<sup>38</sup> and making the assumption that the equilibrium constant<sup>40</sup>  $K_1 \ll 10^{-11}$ , is  $p = 5 \times 10^{-6}$ . This heat treated crystal was measured in R-57. From Fig. 6 it can be seen that this change in vacancy concentration from  $2.6 \times 10^{20} \text{ cm}^{-3}$  in R-37 to  $2 \times 10^{17} \text{ cm}^{-3}$  in R-57 increases the thermal conductivity below 60°K. Crystal R-63 was given a similar anneal at 1620°K in an oxygen pressure of  $2 \times 10^{-6}$  atm. Its vacancy concentration, based on the same calculation as used for pure  $\text{Fe}_3\text{O}_4$ , is about  $8 \times 10^{18} \text{ cm}^{-3}$ .

In view of the high content of chemical impurities and iron vacancies, the effect of the naturally occurring isotopes on the thermal conductivity<sup>41</sup> will be quite small in most of the crystals studied. However the  $\Gamma$  values for the pure crystals containing the normally occurring isotopes<sup>42</sup> are given in Table III. Here  $\Gamma$  for the single element  $A$  is defined by

$$\Gamma(A) = \frac{1}{12} \sum_i f_i \left( \frac{m_i - m_A}{m_A} \right)^2, \quad (1)$$

$$m_A = \sum_i f_i m_i,$$

where  $f_j$  is the fractional concentration of the  $j$ th isotope of mass  $m_j$ . Note that this definition of  $\Gamma$  is the  $B\Gamma$  of reference 41 with  $B = \frac{1}{12}$ . This new definition has also been used in reference 14. The  $\Gamma$  values computed for the individual elements<sup>42</sup> are  $\Gamma(\text{Al}) = 0$ ,  $\Gamma(\text{oxygen}) = 0.28 \times 10^{-5}$ ,  $\Gamma(\text{Fe}) = 0.69 \times 10^{-5}$ ,  $\Gamma(\text{Mg}) = 6.28 \times 10^{-5}$ . For a compound<sup>43</sup>  $A_x B_y C_z$  the composite

<sup>33</sup> G. Hagg, Z. physik. Chem. **B29**, 95 (1935).

<sup>34</sup> S. C. Abrahams and B. A. Calhoun, Acta Cryst. **6**, 105 (1953).

<sup>35</sup> R. W. G. Wyckoff, *Crystal Structures* (Interscience Publishers, Inc., New York, 1948-1960).

<sup>36</sup> E. J. W. Verwey, Z. Krist. Mineral. Petrog. **91**, 65 (1935).

<sup>37</sup> K. P. Sinha and A. P. B. Sinha, J. Phys. Chem. **61**, 758 (1957).

<sup>38</sup> J. W. Greig, E. Posnjak, H. E. Merwin, and R. B. Sosman, Am. J. Sci. **30**, 239 (1935).

<sup>39</sup> L. S. Darken and R. W. Gurry, J. Am. Chem. Soc. **68**, 798 (1946).

<sup>40</sup> H. Flood and D. G. Hill, Z. Elektrochem. **61**, 18 (1957).

<sup>41</sup> G. A. Slack, Phys. Rev. **105**, 829, 832 (1957).

<sup>42</sup> D. Strominger, J. M. Hollander, and G. T. Seaborg, Revs. Modern Phys. **30**, 585 (1958).

<sup>43</sup> The values of  $\Gamma(\text{CaF}_2)$  and  $\Gamma(\text{ZnF}_2)$  in reference 14 were incorrectly computed. They should be a factor of 3 larger in order to account for the 3 atoms per molecule. The  $\Gamma(\text{Ca})$  and  $\Gamma(\text{Zn})$  values are correct.

TABLE III. Parameters for calculating  $\Gamma K_I$ , the thermal conductivity when limited by isotope scattering.<sup>a</sup>

Crystal	$\Gamma \times 10^3$	$\Lambda_0/\Lambda_i^0$	$\theta\Lambda_0/TA_i^0$ (w/cm deg)	$K_I$ (w/cm deg)	$K_{obs}$ (w/cm deg)
MgO	4.66	$5.6 \times 10^3$	$8.6 \times 10^4$	15	15.
MgAl <sub>2</sub> O <sub>4</sub>	1.38	$2.0 \times 10^3$	$3.6 \times 10^4$	45	1.4
Al <sub>2</sub> O <sub>3</sub>	0.10	$0.14 \times 10^3$	$0.27 \times 10^4$	200	59.
Fe <sub>3</sub> O <sub>4</sub>	0.88	$1.5 \times 10^3$	$1.8 \times 10^4$	22	0.95

<sup>a</sup>  $\Gamma$  = isotope scattering parameter.  $\Lambda_0/\Lambda_i^0$  = ratio of mean free paths for phonon-phonon and phonon-isotope scattering (see text).  $K_I$  = calculated thermal conductivity at 50°K when limited only by isotope scattering.  $K_{obs}$  = observed value of the thermal conductivity at 50°K.

$\Gamma$ , denoted by  $\Gamma(A_xB_yC_z)$  is given by

$$\Gamma(A_xB_yC_z) = \frac{x}{(x+y+z)} \left( \frac{m_A}{\bar{m}} \right)^2 \Gamma(A) + \frac{y}{(x+y+z)} \left( \frac{m_B}{\bar{m}} \right)^2 \Gamma(B) + \frac{z}{(x+y+z)} \left( \frac{m_C}{\bar{m}} \right)^2 \Gamma(C),$$

and

$$\bar{m} = (xm_A + ym_B + zm_C)/(x+y+z). \quad (2)$$

This is equivalent to Eq. (12) of Berman, Foster, and Ziman.<sup>44</sup> By using  $(A_xB_yC_z)$  the compound can now be treated as a monatomic material with an average mass  $\bar{m}$  and an average volume per atom  $V_0$ .

Equation (2) is only valid if the atoms  $A$ ,  $B$ ,  $C$  have definite positions in the lattice. This is important, especially in the spinels, since in a random spinel the atoms  $A$  and  $B$  may be distributed randomly on the tetrahedral and octahedral sites. Then the  $\Gamma$  from Eq. (2) would be much too small. The only samples for which such an effect might be important are the MgO·3.5Al<sub>2</sub>O<sub>3</sub>, the Mg<sub>x</sub>Fe<sub>y</sub>Al<sub>2</sub>O<sub>4</sub>, and the Co<sub>0.07</sub>Fe<sub>2.93</sub>O<sub>4</sub>. The Fe<sub>3</sub>O<sub>4</sub> is an inverse spinel where all the cations have the same mass, and the MgAl<sub>2</sub>O<sub>4</sub> is a normal spinel. So Eq. (2) should be valid for these latter crystal as well as for MgO and  $\alpha$ -Al<sub>2</sub>O<sub>3</sub>.

### EXPERIMENTAL TECHNIQUE

The thermal conductivity of the crystals was measured by a steady state heat flow method in a rod-shaped sample. The power input was measured electrically, and the temperature gradient was measured with a gold-cobalt versus manganin differential thermocouple. The exact details have previously been published.<sup>14</sup>

### RESULTS

#### MgO

The present results from 2.9° to 300°K on two single crystals, R-14 and R-38, of MgO are shown in Fig. 1 together with previous data on single crystals from the

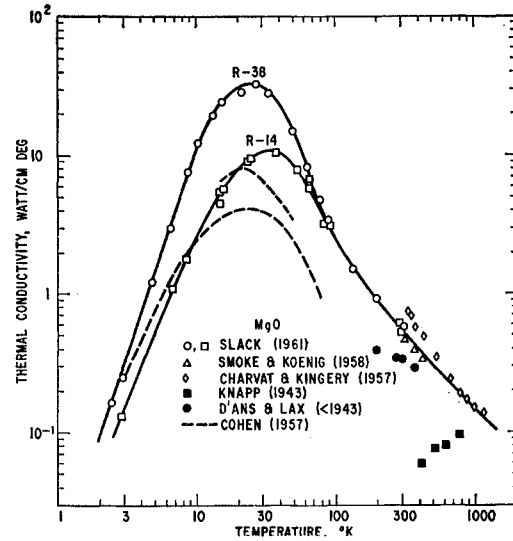


Fig. 1. The thermal conductivity vs temperature of single crystals of MgO. The data of various other authors are also shown.

literature. The agreement with Smoke and Koenig,<sup>45</sup> and with Charvat and Kingery,<sup>46</sup> who made measurements at temperatures above 300°K, is satisfactory. The agreement of the values quoted (from an unknown source) by D'Ans and Lax<sup>47</sup> with the present results is only fair, while Knapp's<sup>48</sup> values are definitely incorrect. Knapp failed to consider thermal contact resistance effects in his temperature gradient measurements. This failure has also been noted by other authors.<sup>49</sup> Some of Cohen's thermal conductivity results at low temperatures on single crystals of MgO from the Norton Company<sup>50</sup> are also shown in Fig. 1. The author wishes to thank her for permission to quote these results, which have previously been mentioned in the literature.<sup>51,52</sup> The upper of the two dotted curves measured by Cohen refers to a crystal with an effective diameter  $d$  of 0.21 cm, and the lower curve to one with  $d=0.51$  cm. These are similar to the  $d$  values given in Table I. The estimated impurity content of Cohen's crystals was kindly furnished, and the dominant impurities were Al, Fe, and Si, all at a concentration of about  $10^{19}$  cm<sup>-3</sup>. These concentrations are somewhat higher than those given in Table II, particularly for

<sup>45</sup> E. J. Smoke and J. H. Koenig, College of Engineering Research Bulletin 40, Rutgers University, New Brunswick, New Jersey 1958 (unpublished).

<sup>46</sup> F. R. Charvat and W. D. Kingery, J. Am. Ceram. Soc. **40**, 306 (1957).

<sup>47</sup> J. D'Ans and E. Lax, *Taschenbuch für Chemiker und Physiker* (Springer-Verlag, Berlin, Germany, 1949), p. 1125.

<sup>48</sup> W. J. Knapp, J. Am. Ceram. Soc. **26**, 48 (1953).

<sup>49</sup> J. Francl and W. D. Kingery, J. Am. Ceram. Soc. **37**(II), 80 (1954).

<sup>50</sup> The Norton Company, Worcester, Massachusetts.

<sup>51</sup> A. F. Cohen and L. C. Templeton, Bull. Am. Phys. Soc. **2**, 188 (1957).

<sup>52</sup> A. F. Cohen, *Low Temperature Physics and Chemistry*, edited by J. R. Dillinger (University of Wisconsin Press, Madison, Wisconsin, 1958), p. 385.

<sup>44</sup> R. Berman, E. L. Foster, and J. M. Ziman, Proc. Roy. Soc. (London) **A237**, 344 (1956).

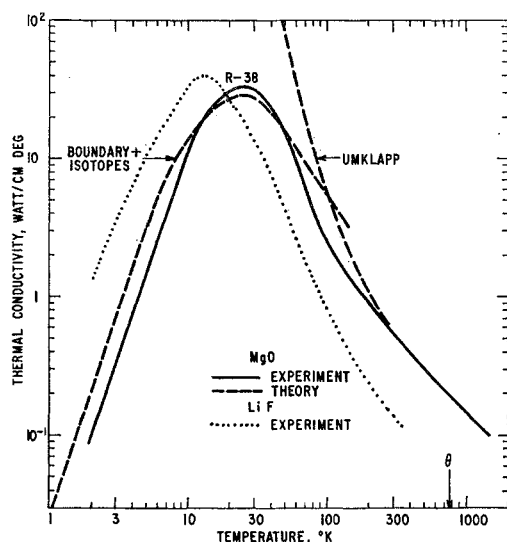


FIG. 2. The thermal conductivity vs temperature of the best MgO crystal compared to the theory. The two dashed curves are the theoretical limits imposed on the phonon heat transport by umklapp scattering, and by a combination of boundary plus isotope scattering. The Debye temperature of MgO is  $\theta$ . A curve for LiF is shown for comparison.

Fe, and probably account for the lower  $K_{\max}$  values found by Cohen.

The curve in Fig. 1 above 300°K also agrees quite well with data<sup>8</sup> on high purity ceramic samples corrected to zero porosity. This is understandable because the particle size of the ceramic is large compared to the average phonon mean free paths for temperatures above 300°K. Therefore the thermal conductivity in both the single crystal and ceramic samples is determined mainly by phonon-phonon scattering.

The results on the crystal with the highest thermal conductivity, R-38, can be compared with theory. This comparison is shown in Fig. 2. The theoretical calculations for MgO as well as for the other crystals will be made by calculating the thermal conductivity at  $T = 10^\circ\text{K}$ ,  $50^\circ\text{K}$ , and  $\theta^\circ\text{K}$ . The curve-fitting-by-machine-computation method of Callaway<sup>53</sup> does not seem appropriate here because the theory of the effects of magnetic impurities and magnetic disorder is not yet well developed. At 10°K the most important phonon scatterers are boundaries or chemical impurities, at 50°K they are isotopes or other mass fluctuations, at  $T = \theta$  they are umklapp processes. The ideal  $K$  vs  $T$  relation for  $0^\circ\text{K} \leq T \leq 100^\circ\text{K}$  is determined on an absolute basis using well-developed theories. For  $100^\circ\text{K} \leq T \leq \theta$  an empirical  $K$  vs  $T$  curve is matched to coincide with  $K_\theta$ , the experimentally determined value of  $K$  at  $T = \theta$ . In those temperature ranges where several scattering processes are equally important approximate averages are used.

For any such calculation it is first necessary to know

<sup>53</sup> J. Callaway, Phys. Rev. **113**, 1046 (1959); *ibid.* **122**, 787 (1961).

some of the physical constants for MgO as shown in Table IV. Using these constants a theoretical value  $K_\theta'$  for the thermal conductivity at the Debye temperature  $\theta$  can be calculated using the theory of Leibfried and Schlömann.<sup>54</sup> Assuming the crystal is monatomic, and using the average values of  $M$ ,  $\theta$ ,  $V_0$  with their units as listed in Table IV, this theory gives

$$K_\theta' = 5.72 \times 10^{-8} (M\theta^2 V_0^{1/3} \gamma^{-2}) \text{ w/cm deg}, \quad (3)$$

where  $\theta$  is the value at 300°K. The Grüneisen constant  $\gamma$  is taken to be equal to 2.0 for all of the crystals. The value for MgO at 300°K as calculated from the elastic constants,<sup>55</sup> the specific heat,<sup>56,57</sup> and the thermal expansion,<sup>58</sup> is  $\gamma = 1.54$ . Since  $K_\theta'$  is being used mainly for comparison of the various crystals, since the  $\gamma$  values for most of them are not known, and since the experimental value of  $\gamma$  is not necessarily the correct one<sup>59</sup> to use in the theory for  $K_\theta'$ ,  $\gamma = 2.0$  seems to be a satisfactory choice. With this choice of variables, the  $K_\theta'$  values for the four crystals  $\text{Al}_2\text{O}_3$ ,  $\text{MgAl}_2\text{O}_4$ ,  $\text{Fe}_3\text{O}_4$ , and MgO all lie between 0.54 and 0.35 w/cm deg, and decrease in this order. This very nearly reflects the variation in  $\theta$ . In the last column of Table IV, the  $K_\theta$  values are listed. The  $K_\theta$  show a greater range of values than do the  $K_\theta'$ . The closest agreement between the computed  $K_\theta'$  and the experimental  $K_\theta$  is for MgO, which has the simple NaCl crystal structure, where  $K_\theta/K_\theta' = 0.57$ . This lattice has very high symmetry, as does the fcc lattice used in the theoretical computation<sup>54</sup> of  $K_\theta'$ . The  $\text{MgAl}_2\text{O}_4$  is also cubic, but possesses a lower symmetry than MgO. The  $\text{Al}_2\text{O}_3$  is not cubic, but rather has a rhombohedral structure. The ratio  $K_\theta/K_\theta' = 0.15$  for these two crystals. The general behavior is that crystals of low symmetry appear to have  $K_\theta$  values lower than crystals of high symmetry.

Over the whole temperature range studied in MgO phonons are by far the dominant carriers of thermal energy. As can be seen from Fig. 2 the experimental results on the highest conductivity crystal, R-38, can be explained by invoking only three main scattering processes. These are boundary scattering,<sup>60</sup> isotope scattering,<sup>41</sup> and umklapp scattering.<sup>54,61</sup> So far the magnitude of the umklapp scattering has been used to calculate  $K_\theta'$  which agrees reasonably well with  $K_\theta$ . The theory of umklapp scattering has not been developed to the point where the variation in  $K$  with temperature for  $T < \theta$  can be calculated. Leibfried and Schlömann<sup>54</sup> have suggested that  $K_u/K_\theta$ , where  $K_u$  is

<sup>54</sup> G. Leibfried and E. Schlömann, Nachr. Akad. Wiss. Göttingen, Math.-physik. Kl. 4, 71 (1954).

<sup>55</sup> M. A. Durand, Phys. Rev. **50**, 449 (1936).

<sup>56</sup> W. F. Giaque and R. C. Archibald, J. Am. Chem. Soc. **59**, 561 (1937).

<sup>57</sup> T. H. K. Barron, W. T. Berg, and J. A. Morrison, Proc. Roy. Soc. (London) **A250**, 70 (1959).

<sup>58</sup> S. S. Sharma, Proc. Indian Acad. Sci. **A32**, 268 (1950).

<sup>59</sup> T. H. K. Barron, Nature **178**, 871 (1956); Ann. Phys. **1**, 77 (1957).

<sup>60</sup> H. B. Casimir, Physica **5**, 495 (1938).

<sup>61</sup> R. E. Peierls, Ann. Physik **3**, 1055 (1929).

TABLE IV. Physical properties of some oxide crystals and values of  $K_\theta$  and  $K_\theta'$ .<sup>a</sup>

Crystal	$V_0$ (Å <sup>3</sup> )	$M$ (g)	$\rho$ (g/cm <sup>3</sup> )	$\bar{v}_\theta$ (10 <sup>6</sup> cm/sec)	$\theta_0$ (°K)	$\theta$ (°K)	$K_\theta'$ (w/cm deg)	$K_\theta$ w/cm deg
MgO	9.35	20.16	3.58	7.0 <sup>b</sup>	949 <sup>b,e</sup>	760 <sup>h</sup>	0.35	0.20
MgAl <sub>2</sub> O <sub>4</sub>	9.42	20.33	3.58	(7.0)	(900)	900 <sup>i</sup>	0.50	0.080
Al <sub>2</sub> O <sub>3</sub>	8.47	20.39	3.99	6.6 <sup>c</sup>	1010 <sup>f</sup>	950 <sup>f</sup>	0.54	0.080
Fe <sub>3</sub> O <sub>4</sub>	10.58	33.08	5.19	2.5 <sup>d</sup>	660 <sup>g</sup>	600 <sup>j</sup>	0.37	(0.06)

<sup>a</sup>  $V_0$ =average volume per atom,  $M$ =average atomic weight per atom,  $\rho$ =x-ray density of crystal,  $\bar{v}_\theta$ =average sound velocity,  $\theta_0$ =Debye temperature at 0°K,  $\theta$ =Debye temperature at 300°K,  $K_\theta'$ =value of thermal conductivity at  $T=\theta$  calculated from Eq. (3),  $K_\theta$ =experimental value of thermal conductivity at  $T=\theta$ , ( )=an approximate value.

<sup>b</sup> See references 55, 57.

<sup>c</sup> J. B. Wachtman, W. E. Teft, D. G. Lam, and R. P. Stinchfield, J. Research Natl. Bur. Standards **64A**, 213 (1960).

<sup>d</sup> M. S. Doraiswamy, Proc. Indian Acad. Sci. **A25**, 413 (1947); M. E. Fine and N. T. Kenney, Phys. Rev. **94**, 1573 (1954); H. J. McSkimin, A. J. Williams, R. M. Bozorth, Phys. Rev. **95**, 616 (1954); see also reference 93.

<sup>e</sup> J. deLaunay, J. Chem. Phys. **24**, 1071 (1956).

<sup>f</sup> G. T. Furukawa, T. B. Douglas, R. E. McCoskey, and D. C. Ginnings, J. Research Natl. Bur. Standards **57**, 67 (1956).

<sup>g</sup> J. S. Kouvel, Phys. Rev. **102**, 1489 (1956).

<sup>h</sup> See reference 57.

<sup>i</sup> E. G. King, J. Phys. Chem. **59**, 218 (1955).

<sup>j</sup> See reference 17; G. S. Parks and K. K. Kelley, J. Phys. Chem. **30**, 47 (1926).

the thermal conductivity determined only by umklapp scattering, should be a "universal function" of reduced temperature  $T/\theta$ . An empirical function of this nature has been constructed by Slack<sup>14</sup> from a combination of the thermal conductivity data on isotopically clean (or nearly so)  $\alpha$ -Al<sub>2</sub>O<sub>3</sub>, H<sub>2</sub>, He<sup>4</sup>, and He<sup>3</sup>. This "universal function" has been matched to the MgO curve in Fig. 2 at  $T=\theta$ , and is shown as the dashed umklapp curve. From the comparison of the umklapp curve  $K_u$  with the experimental one in Fig. 2 it can be seen that umklapp scattering is dominant for  $100^\circ\text{K} \leq T \leq 1400^\circ\text{K}$ , is important for  $50^\circ\text{K} \leq T \leq 100^\circ\text{K}$ , and is negligible for  $T \leq 50^\circ\text{K}$ . The difference between the umklapp and experimental curves for  $50^\circ\text{K} \leq T \leq 300^\circ\text{K}$  is attributable mainly to isotope scattering.

The theoretical calculation of isotope scattering has been studied by Klemens,<sup>62,63</sup> Callaway and von Baeyer,<sup>63,64</sup> and Berman *et al.*<sup>65</sup> Of these the variational method of Ziman in Berman *et al.* is favored here. It agrees<sup>64</sup> with the more involved computation by Callaway. Provided that the dimensionless parameter  $\theta\Lambda_0/TA_i^0$  lies in the range  $10^3$  to  $10^7$ , the thermal conductivity for  $T/\theta \ll 1$  is given<sup>14,65</sup> approximately by

$$K_I = 0.055 k^{3/2} M^{1/2} \gamma^{-1} N_A^{-1/2} (\Gamma^{-1/2} T^{-3/2}), \quad (4)$$

where  $k$ =Boltzmann's constant,  $h$ =Planck's constant,  $N_A$ =Avogadro's number, and where boundary and umklapp scattering can be neglected. For a temperature of  $T=50^\circ\text{K}$  the calculated value for  $K_I$  for MgO as well as of the other crystals is given in Table III. The parameter  $\Lambda_0/\Lambda_i^0$  has been calculated from

$$\Lambda_0/\Lambda_i^0 = 7.08 \times 10^3 \theta M \Gamma V_0^{1/3} \gamma^{-2}. \quad (5)$$

$\Gamma$  is given in Table III, and  $\theta$ ,  $M$ , and  $V_0$  with their units in Table IV, and  $\gamma=2.0$ . The parameter  $\Lambda_0/\Lambda_i^0$

is equal to

$$\frac{\Lambda_0}{\Lambda_i^0} = 2.5 \times 10^4 \left( \frac{\text{phonon m.f.p. for umklapp scattering}}{\text{phonon m.f.p. for isotope scattering}} \right)$$

evaluated at  $T=\theta$  for phonons of frequency  $\nu=(k\theta/h)$ . The ratio  $\Lambda_u^0/\Lambda_i^0$  given by Ziman in his book<sup>66</sup> is just the above factor in the parentheses ( ). He has changed the definitions of both  $\Lambda$ 's so as to eliminate the factor of  $2.5 \times 10^4$ . From Table III it can be seen that  $\theta\Lambda_0/TA_i^0$  is in the appropriate range at  $50^\circ\text{K}$  so that Eq. (4) is valid for all of the crystals. The calculated value of  $K_I$  at  $50^\circ\text{K}$  for MgO is in good agreement with the observed value, as can be seen from Table III and also from Fig. 2. This very good agreement is somewhat fortuitous because crystal R-38 still has an over-all impurity concentration of about  $2 \times 10^{19}/\text{cm}^{-3}$ , as shown in Table II. If these impurities were eliminated, it is estimated that the maximum thermal conductivity at  $25^\circ\text{K}$  might increase by a factor of 2.

From Fig. 2 it can be seen that the curve for R-38 comes close to the thermal conductivity limit imposed by boundary scattering for  $T < 5^\circ\text{K}$ . The dashed curve labeled "boundary+isotopes" was computed by graphically combining (a) the low temperature effects of boundary and isotope scattering calculated using the method of Slack and Glassbrenner<sup>67</sup> with (b) the isotope scattering calculated from Eq. (4). It was assumed that the pure boundary scattering for  $T < 5^\circ\text{K}$  was for a perfectly diffuse scattering of phonons from the crystal surface. Hence the mean free path is equal to the sample diameter  $d$  in Table I. The fact that the thermal conductivity is lower than the boundary limit is attributed to the effects of the residual chemical impurities. This rather pronounced effect of impurities at temperatures below the maximum in the  $K$  vs  $T$  curve has been noticed before in other crystals by

<sup>62</sup> P. G. Klemens, Proc. Phys. Soc. (London) **A68**, 1113 (1955).

<sup>63</sup> P. G. Klemens, Proc. Phys. Soc. (London) **A70**, 833 (1957).

<sup>64</sup> J. Callaway and H. C. von Baeyer, Phys. Rev. **120**, 1149 (1960).

<sup>65</sup> R. Berman, P. T. Nettle, F. W. Sheard, A. N. Spencer, R. W. H. Stevenson, and J. M. Ziman, Proc. Roy. Soc. (London) **A253**, 403 (1959).

<sup>66</sup> J. M. Ziman, *Electrons and Phonons* (Oxford University Press, New York, 1960), p. 311.

<sup>67</sup> G. A. Slack and C. Glassbrenner, Phys. Rev. **120**, 782 (1960).

Slack,<sup>10,14,41</sup> Pohl,<sup>68</sup> Rosenberg and Sujak,<sup>69</sup> Keyes,<sup>70</sup> and Klein.<sup>71</sup> This effect of impurities can be seen in Fig. 1 for crystal R-14 where the maximum  $K$  is lower than in R-38, and where the  $K$  at 3°K is a factor of 6 below the boundary scattering limit. Crystal R-14 is less "pure" than R-38. The major difference between the impurities in R-14 and R-38 that would cause this  $K$  difference would seem to be the Si and Zr listed in Table II. These might be expected to fit less well into the MgO lattice than the Ca and Al impurities which, incidentally, are more prevalent in R-38 than in R-14.

The general result for MgO is that crystal R-38 is sufficiently free of chemical impurities so that its thermal conductivity approaches the theoretical limits. A comparison of the results for MgO in R-38 with data for the alkali halide LiF is instructive. A composite curve of  $K$  versus  $T$  for a single crystal of LiF with a diameter of 0.79 cm and with the Li and F isotopes present in their natural abundances<sup>42</sup> is shown dotted in Fig. 2. This curve has been constructed using the data available in the literature.<sup>44,65,72-74</sup> The two curves have very nearly the same shape. The thermal conductivity ratio at some chosen temperature is denoted by  $[K(\text{MgO})/K(\text{LiF})]$ . Experimentally this ratio is 0.1 from 2° to 10°K, and from 30° to 300°K is nearly constant at a value of 3 to 4. MgO and LiF both have the cubic NaCl structure, and have similar phonon spectra.<sup>57</sup> Their main differences in  $K$  should be caused by  $M$ ,  $\theta$ ,  $V_0$ ,  $\Gamma$ , and  $d$ , and perhaps by the fact that MgO is a divalent crystal while LiF is monovalent. From 2° to 10°K the thermal conductivity  $K_B$  is determined by boundary scattering for both crystals. For LiF  $d = 0.79$  cm,  $V_0 = 8.06$  Å<sup>3</sup>,  $\theta_0 = 743^\circ\text{K}$ .<sup>75</sup> Thus from 2° to 10°K the calculated ratio is  $[K_B(\text{MgO})/K_B(\text{LiF})] = 0.2$  compared to the observed 0.1.

From 30° to 60°K the thermal conductivity is determined by isotope scattering. For LiF  $M = 12.97$  g, and  $\Gamma$  has a value<sup>42</sup> of  $\Gamma = 1.70 \times 10^{-5}$ . This yields a calculated value of  $[K_I(\text{MgO})/K_I(\text{LiF})] = 1.6$ . For  $T > 200^\circ\text{K}$  the conductivity  $K_u$  is determined by umklapp scattering, and at temperatures near and above  $T = \theta$  one has  $K_u = (\theta/T)K_\theta$ . This means that for  $T > 200^\circ\text{K}$  the calculation gives  $[K(\text{MgO})/K(\text{LiF})] = 3.4$ , which is only twice the value computed at lower temperatures. For both  $K_I$  and  $K_u$  a value of  $\gamma = 2$  has been assumed for LiF and MgO. The general agreement of the computed ratio from 30° to 300°K with the observed one of 3 to 4 indicates that there is no appreciable difference

in the application of the theory to monovalent or divalent crystals. The conclusion is that in the application of the same theory to  $\text{Al}_2\text{O}_3$ ,  $\text{MgAl}_2\text{O}_4$ , and  $\text{Fe}_3\text{O}_4$  no explicit account of the various valences need be taken.

### $\alpha\text{-Al}_2\text{O}_3$

Many previous measurements of the thermal conductivity of  $\alpha\text{-Al}_2\text{O}_3$  have been made, and therefore such measurements were not repeated in the present series of experiments. A  $K$  vs  $T$  curve for single crystals has been constructed from the results of Berman *et al.*<sup>76</sup> from 3° to 93°K, Berman<sup>77</sup> from 3° to 200°K, Ballard and McCarthy<sup>78</sup> from 300° to 350°K, Smoke and Koenig<sup>45</sup> from 315° to 420°K, Weeks and Seifert<sup>79</sup> at 340°K, Lee and Kingery<sup>80</sup> from 330° to 1300°K, Kingery *et al.*<sup>8</sup> from 370° to 2070°K, and Charvat and Kingery<sup>46</sup> from 500° to 1500°K. The anisotropy in  $K$  for these rhombohedral crystals of  $\alpha\text{-Al}_2\text{O}_3$  has been measured accurately by Smoke and Koenig<sup>45</sup> who obtained 1.08 for the ratio of  $K_c$ , measured along the  $c$  axis, to  $K_a$ , measured in the  $a$ - $b$  plane. Jannettaz<sup>81</sup> found  $K_c/K_a = 1.18$ , while the results of Ballard and McCarthy<sup>78</sup> give 1.11 at 300°K. Since this anisotropy is small, it has been neglected in determining the resultant curve.

The composite  $K$  vs  $T$  curve for  $\alpha\text{-Al}_2\text{O}_3$  is shown in Fig. 3 together with the data for the highest conductivity samples of MgO and  $\text{MgAl}_2\text{O}_4$ . The experimental curve for  $\alpha\text{-Al}_2\text{O}_3$  is reasonably well explained by assuming that only umklapp scattering<sup>14</sup> and boundary scattering<sup>76</sup> are important. The  $K$ , as limited by isotope scattering, is shown in Table III for  $\text{Al}_2\text{O}_3$  for 50°K. Previous authors<sup>41,44</sup> have pointed out that the isotope scattering in  $\alpha\text{-Al}_2\text{O}_3$  can be neglected. Since many of the  $K$  measurements<sup>46,76,78,79</sup> have been made on Linde<sup>22</sup> crystals, a spectrographic analysis of a random piece of Linde  $\alpha\text{-Al}_2\text{O}_3$  crystal was made. The most abundant chemical impurities found were Na and Si at about  $1 \times 10^{18}$  cm<sup>-3</sup>. Thirteen other common metallic impurities were checked for and, if present, were each  $\leq 5 \times 10^{17}$  cm<sup>-3</sup>. This low concentration of chemical impurities accounts for the fact that the expected exponential rise in  $K$  at low temperatures can be observed.

The main differences in the curves for MgO and  $\alpha\text{-Al}_2\text{O}_3$  in Fig. 3 are caused by crystal symmetry effects which make  $K(\text{MgO}) > K(\text{Al}_2\text{O}_3)$  for  $300^\circ\text{K} \leq T \leq 1500^\circ\text{K}$ , and by isotope scattering in the MgO which makes  $K(\text{MgO}) < K(\text{Al}_2\text{O}_3)$  for  $30^\circ\text{K} \leq T \leq 100^\circ\text{K}$ .

<sup>68</sup> R. O. Pohl, Phys. Rev. **118**, 1499 (1960).

<sup>69</sup> H. M. Rosenberg and B. Sujak, Phil. Mag. **5**, 1299 (1960).

<sup>70</sup> R. W. Keyes, Phys. Rev. **122**, 1171 (1961).

<sup>71</sup> M. V. Klein, Phys. Rev. **122**, 1393 (1961); *ibid.* **123**, 1977 (1961).

<sup>72</sup> S. S. Ballard, K. A. McCarthy, and W. C. Davis, Rev. Sci. Instr. **21**, 905 (1950).

<sup>73</sup> R. Srinivasan, J. Indian Inst. Sci. **A37**, 200 (1955).

<sup>74</sup> R. L. Sproull, M. Moss, and H. Weinstock, J. Appl. Phys. **30**, 334 (1959).

<sup>75</sup> T. H. K. Barron and J. A. Morrison, Can. J. Phys. **35**, 799 (1957).

<sup>76</sup> R. Berman, E. L. Foster, and J. M. Ziman, Proc. Roy. Soc. (London) **A231**, 130 (1955).

<sup>77</sup> R. Berman, Proc. Phys. Soc. (London) **A65**, 1029 (1952).

<sup>78</sup> S. S. Ballard and K. A. McCarthy, J. Opt. Soc. Am. **41**, 1062 (1951).

<sup>79</sup> J. L. Weeks and R. L. Seifert, Rev. Sci. Instr. **24**, 1054 (1953).

<sup>80</sup> D. W. Lee and W. D. Kingery, J. Am. Ceram. Soc. **43**, 594 (1960).

<sup>81</sup> E. Jannettaz, Compt. rend. **114**, 1352 (1892).



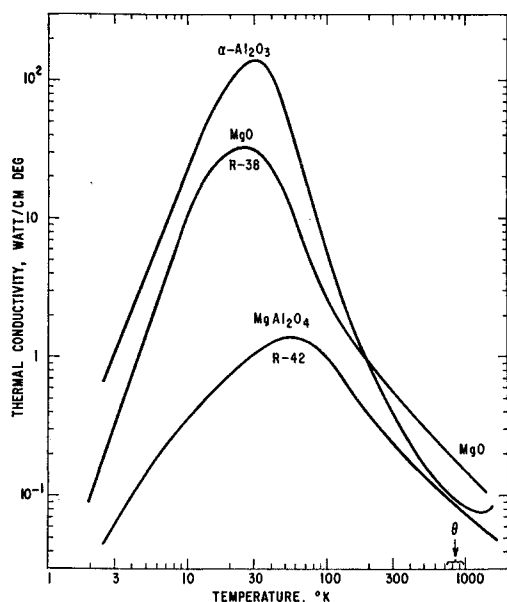


FIG. 3. A comparison of the experimental results of thermal conductivity vs temperature for the best crystals of  $\alpha$ -Al<sub>2</sub>O<sub>3</sub>, MgO, and MgAl<sub>2</sub>O<sub>4</sub>. All three Debye temperatures,  $\theta$ , fall within the range indicated.

### MgAl<sub>2</sub>O<sub>4</sub>

Two natural crystals of MgAl<sub>2</sub>O<sub>4</sub> were measured, and the results are shown in Fig. 3. These crystals, R-42 and R-54, have very nearly the same thermal conductivity from 100° to 300°K. At 300°K the value of  $K = 0.24$  w/cm deg. The only previous results in the literature on MgAl<sub>2</sub>O<sub>4</sub> are some by Anderson<sup>82</sup> on ceramic samples from 370° to 1050°K. The agreement between the ceramic samples and the single crystals is quite good, as can be seen in Fig. 4.

The analysis of the results on MgAl<sub>2</sub>O<sub>4</sub> in terms of the simple theory used for the MgO is not very satisfactory because the crystals are quite impure. The total impurity content, as given in Table II, is about  $0.6 \times 10^{20}$  cm<sup>-3</sup> for R-42 and  $1 \times 10^{20}$  cm<sup>-3</sup> for R-54. That is, 0.2% of the metal atoms in the crystal are foreign atoms. This concentration of impurities, however, will not have much effect on the value of  $K_\theta$ , which is 0.080 w/cm deg, and is listed in Table IV. Thus MgAl<sub>2</sub>O<sub>4</sub> will serve as a useful guide to estimate  $K_\theta$  for Fe<sub>3</sub>O<sub>4</sub>. It is assumed that the experimental to theoretical ratio  $K_\theta/K_\theta'$  for Fe<sub>3</sub>O<sub>4</sub> is the same as for MgAl<sub>2</sub>O<sub>4</sub> since they both have the same crystal structure and somewhat similar atomic masses. This assumption leads to  $K$  for Fe<sub>3</sub>O<sub>4</sub> of 0.06 w/cm deg, which is not an implausible extrapolation of the curve in Fig. 8.

The umklapp and boundary scattering limits have been computed in the same manner as they were for MgO. These limits are shown in Fig. 4. The experi-

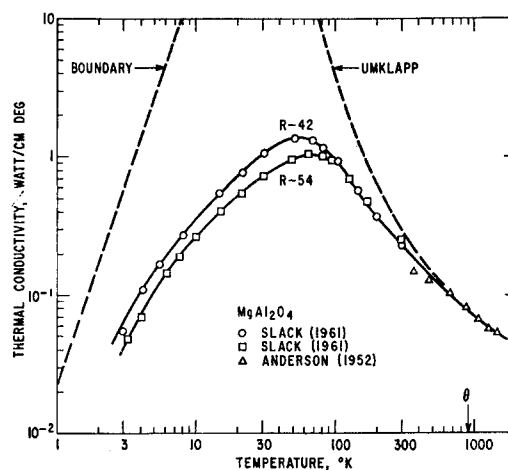


FIG. 4. The thermal conductivity vs temperature of two natural crystals of MgAl<sub>2</sub>O<sub>4</sub>. The data above 300°K by Anderson are for a ceramic sample. The dashed curves are the theoretical limits calculated for umklapp scattering and boundary scattering.

mental curve of  $K$  vs  $T$  begins to fall markedly below these limits for  $T < 200^\circ\text{K}$ . Notice that the limit on  $K$  imposed by isotope scattering in Table III is 45 w/cm deg at 50°K. This limit falls way above the graph in Fig. 4.

### Impurities in MgAl<sub>2</sub>O<sub>4</sub>

Of the impurities listed in Table II for R-42 and R-54 the V, Ti, Cr, and Fe impurities may be the ones most responsible for the low thermal conductivity at low temperatures. It can be concluded that certain paramagnetic impurities can have a large effect on  $K$  at low temperatures from the results of Rosenberg and Sujak.<sup>69</sup> Since neither the charge state nor the lattice environment of these trace impurities in the present samples is known, let us consider first the total content per cm<sup>3</sup> of the transition metal impurities that are listed as present in Table II. Denote this total concentration as  $C_1$ . For R-42  $C_1 = 4 \times 10^{19}$  cm<sup>-3</sup>, and for R-54  $C_1 = 6 \times 10^{19}$  cm<sup>-3</sup>. The total concentration of nontransition metal impurities is denoted by  $C_2$ . The  $C_2$  values are  $1 \times 10^{20}$  cm<sup>-3</sup> for R-42 and  $4 \times 10^{19}$  for R-54. Zinc accounts for at least 80% of these  $C_2$  values. However, this high concentration of Zn in both crystals will not affect the thermal conductivity appreciably because the Zn enters the tetrahedral sites in place of the Mg and essentially forms a mixed crystal of MgAl<sub>2</sub>O<sub>4</sub>-ZnAl<sub>2</sub>O<sub>4</sub>. Both of these are normal spinels of nearly the same lattice parameter, so that the phonon scattering by the Zn is mainly due to the mass difference. The effect of this small amount of Zn (0.2%) on the thermal conductivity is thus<sup>83,84</sup> quite small. For example  $\Gamma = 4 \times 10^{-4}$  due to the mass fluctuation produced by the Zn in R-42. It will be noticed later in

<sup>82</sup> As quoted in reference 8.

<sup>83</sup> W. S. Williams, Phys. Rev. **119**, 1021 (1960).

<sup>84</sup> A. M. Toxen, Phys. Rev. **122**, 450 (1961).

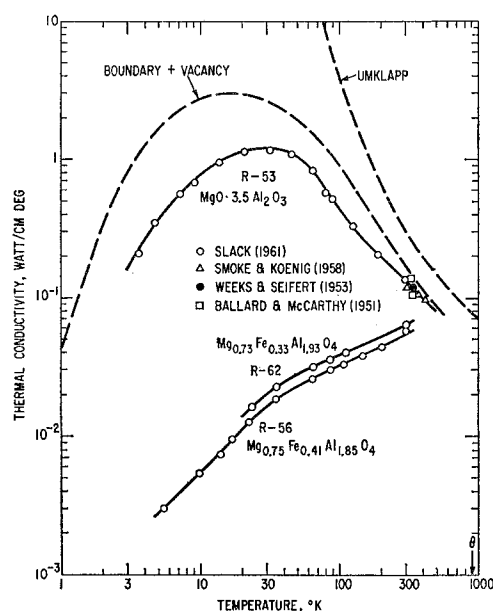


Fig. 5. The thermal conductivity vs temperature of a synthetic  $\text{MgO} \cdot 3.5 \text{Al}_2\text{O}_3$  spinel crystal and two natural  $\text{Mg}_x\text{Fe}_{1-x}\text{Al}_2\text{O}_4$  crystals. The literature data are for synthetic spinel. The dashed curves are the theoretical limits for the synthetic spinel computed for boundary, vacancy, and umklapp scattering.

Fig. 9 that the "best-fit" thermal resistivity versus concentration curve passes close to the transition metal concentration  $C_1$  for both R-42 and R-54. This agrees with the present conclusion that the transition metal impurities rather than the Zn are primarily responsible for the low thermal conductivity for  $T < 50^\circ\text{K}$ .

The  $K$  versus  $T$  curve for R-42 is also plotted in Fig. 3. At temperatures above  $300^\circ\text{K}$  the  $K$  of  $\text{MgAl}_2\text{O}_4$  is nearly the same as that for  $\alpha\text{-Al}_2\text{O}_3$ , and both of these are lower than  $\text{MgO}$ , probably for symmetry reasons as previously mentioned. For temperatures  $3^\circ\text{K} \leq T \leq 300^\circ\text{K}$  the high concentration of transition metal impurities in the  $\text{MgAl}_2\text{O}_4$  is responsible for the fact that its thermal conductivity is much less than either that of  $\text{MgO}$  or  $\alpha\text{-Al}_2\text{O}_3$ . If the crystal boundaries and the naturally occurring isotopes in  $\text{MgAl}_2\text{O}_4$  were the chief limitation on its thermal conductivity at low temperatures, then its  $K$  vs  $T$  curve in Fig. 3 should lie between those for  $\text{MgO}$  and  $\alpha\text{-Al}_2\text{O}_3$ . Therefore it is concluded that the thermal conductivity of the pure double oxide  $\text{MgAl}_2\text{O}_4$  is not significantly different from what would have been predicted by a crude arithmetic average of the results for the single constituent oxides  $\text{MgO}$  and  $\alpha\text{-Al}_2\text{O}_3$ .<sup>84a</sup>

### Grossly Impure $\text{MgAl}_2\text{O}_4$

Since  $\text{Fe}_3\text{O}_4$  crystals can possess large concentrations of chemical impurities or vacancies, it is instructive to

see what effect such large concentrations have on the thermal conductivity of  $\text{MgAl}_2\text{O}_4$ . For this purpose  $K$  measurements were made on crystals of  $\text{Mg}_x\text{Fe}_{1-x}\text{Al}_2\text{O}_4$  and  $\text{MgO} \cdot 3.5\text{Al}_2\text{O}_3$ . The first contains a large number of Fe impurities, and the second metal ion vacancies, but both have essentially the same crystal structure and lattice dynamics as the parent  $\text{MgAl}_2\text{O}_4$ . Figure 5 shows the results on  $\text{Mg}_x\text{Fe}_{1-x}\text{Al}_2\text{O}_4$  (R-56 and R-62), and  $\text{MgO} \cdot 3.5\text{Al}_2\text{O}_3$  (R-53). The agreement of the results on R-53 with previous data on similar single crystals by Smoke and Koenig,<sup>45</sup> Weeks and Seifert,<sup>79</sup> and Ballard and McCarthy<sup>78,85</sup> is good. The analysis of these results in terms of umklapp, isotope, and boundary scattering is very nearly the same as for  $\text{MgAl}_2\text{O}_4$ , and will not be repeated. Assuming  $\theta = 900^\circ\text{K}$ , the same as for  $\text{MgAl}_2\text{O}_4$ , the umklapp limit and pure boundary scattering limit ( $T \leq 2^\circ\text{K}$ ) are given in Fig. 5.

The most noticeable feature for R-56 (and similarly for R-62) is that its thermal conductivity at  $300^\circ\text{K}$ ,  $K = 0.055 \text{ w/cm deg}$ , is 0.23 of that for  $\text{MgAl}_2\text{O}_4$ , and that  $K$  continuously decreases with decreasing temperature. These samples were quite good natural single crystals, and were free of flaws and inclusions. The low value of  $K$  can only be attributed to the large concentration of  $\text{Fe}^{2+}$  impurity. Since  $\text{FeAl}_2\text{O}_4$  is a normal spinel<sup>86</sup> as is  $\text{MgAl}_2\text{O}_4$ , the  $\text{Fe}^{2+}$  in  $\text{Mg}_x\text{Fe}_{1-x}\text{Al}_2\text{O}_4$  probably occurs on the tetrahedral sites.

The distribution of the Fe impurity in the  $\text{Mg}_x\text{Fe}_{1-x}\text{Al}_2\text{O}_4$  can be estimated from Miller's<sup>18</sup> calculations. The result is for R-56 is  $\text{Fe}_{0.41}\text{Mg}_{0.60}[\text{Mg}_{0.15}\text{Al}_{1.85}]_4\text{O}_4$ . The mass fluctuation parameter  $\Gamma$  for this distribution is calculated to be  $\Gamma = 5.9 \times 10^{-3}$ . At temperatures above  $30^\circ\text{K}$  some thermal resistance is provided by this mass fluctuation. By comparison with the following analysis on  $\text{MgO} \cdot 3.5\text{Al}_2\text{O}_3$  a value of  $\Gamma = 5.9 \times 10^{-3}$  leads to a noticeable reduction in  $K$  only at high temperatures. At  $500^\circ\text{K}$  the value of  $K$  for R-56 is calculated as  $0.07 \text{ w/cm deg}$ . This value would be reasonable extrapolation of the results for R-56 in Fig. 4. At  $300^\circ\text{K}$  and below, the mass fluctuation scattering cannot be the explanation of the low thermal conductivity in R-56 or R-62.

The most plausible reason for the low thermal conductivity in R-56 is suggested by Orbach's<sup>87</sup> analysis of Fe-doped  $\text{ZnSO}_4 \cdot 7\text{H}_2\text{O}$ .<sup>69</sup> In this latter crystal the  $\text{Fe}^{2+}$ , which has a  $3d^6$  configuration, is surrounded by six  $\text{H}_2\text{O}$  molecules which produce a tetragonal environment with a slight orthorhombic distortion. Orbach assumes that there is a low lying orbital doublet which is split by the orthorhombic distortion into two levels separated by a small energy  $k\Delta$ , where  $\Delta = 4^\circ\text{K}$ . In the spinel lattice, the four oxygen ions around the tetrahedral site form an undistorted tetrahedron. The tetra-

<sup>85</sup> S. S. Ballard and K. A. McCarthy, *American Institute of Physics Handbook*, edited by D. E. Gray (McGraw-Hill Book Company, Inc., New York, 1957), p. 4-76.

<sup>86</sup> T. F. W. Barth and E. Posnjak, *Z. Krist.* **82**, 325 (1932).

<sup>87</sup> R. Orbach, *Phil. Mag.* **5**, 1303 (1960).

<sup>84a</sup> Note added in proof. Recent measurements on a higher purity synthetic sample of  $\text{MgAl}_2\text{O}_4$  gave a maximum value of  $K$  of  $4.5 \text{ w/cm deg}$  at  $30^\circ\text{K}$ .

hedron remains undistorted even if the oxygen parameter  $u$  is different from 0.375. For MgAl<sub>2</sub>O<sub>4</sub>,  $u = 0.387$ ,<sup>21</sup> and for FeAl<sub>2</sub>O<sub>4</sub>,  $u = 0.390$ .<sup>86</sup> The energy level scheme of Fe<sup>2+</sup> in various crystalline fields is given by McClure.<sup>88</sup> In the tetrahedral field, the orbital doublet is lower than the triplet. The first five electrons half fill the  $d$  shell. The sixth electron goes into the lower energy doublet state producing a twofold degeneracy. This doublet of Fe<sup>2+</sup> in MgAl<sub>2</sub>O<sub>4</sub> may be split by spin-orbit interactions.<sup>89</sup> However, the level separation  $\Delta$  is not yet known for this case. Thus MgAl<sub>2</sub>O<sub>4</sub> and ZnSO<sub>4</sub>·7H<sub>2</sub>O both appear to possess a nearly degenerate doublet ground state for Fe<sup>2+</sup>. Some comparison of the thermal conductivity data can be made. For a ZnSO<sub>4</sub>·7H<sub>2</sub>O crystal with  $C_1 = 2.9 \times 10^{20}$  cm<sup>-3</sup> of Fe<sup>2+</sup>, Rosenberg and Sujak<sup>69</sup> measured the thermal resistivity at 10°K,  $W(10^\circ\text{K})$ , 13.3 cm deg/w.  $W$  varied as  $\sim T^{+0.5}$ . The ratio  $[W(10^\circ\text{K})/C_1] = 4.6 \times 10^{-20}$  cm<sup>4</sup> deg/w. In the present case  $C_1 = 6.1 \times 10^{21}$  cm<sup>-3</sup> for R-56 and  $4.9 \times 10^{21}$  cm<sup>-3</sup> for R-62. Therefore  $[W(10^\circ\text{K})/C_1] = 3 \times 10^{-20}$  cm<sup>4</sup> deg/w for R-56, and one obtains a similar extrapolated value for R-62 from Fig. 5. At 10°K the value of  $W$  varied as  $T^{-1}$ .

The close agreement of these two results on entirely different crystals is probably fortuitous, especially since  $W$  has a different temperature dependence in the two cases. However the agreement of the two  $[W(10^\circ\text{K})/C_1]$  values to within an order of magnitude tends to indicate that the Fe<sup>2+</sup> scattering process is similar in both cases.

In the temperature region between 100° and 500°K the  $K$  of MgO·3.5Al<sub>2</sub>O<sub>3</sub> is noticeably lower than that of MgAl<sub>2</sub>O<sub>4</sub>. This difference is clearly not caused by chemical impurities since the natural MgAl<sub>2</sub>O<sub>4</sub> crystals are less pure than the synthetic MgO·3.5Al<sub>2</sub>O<sub>3</sub>. The difference appears to be caused by vacancies. Not all of the metal ion sites in the spinel lattice are occupied by the metal ions in MgO·3.5Al<sub>2</sub>O<sub>3</sub>. Vacancies occur, and these are probably on the octahedral sites.<sup>87</sup> [Even if the vacancies are on the tetrahedral sites or are distributed at random, the numerical values in the following argument will not be appreciably altered.] Thus for each 4 oxygen O<sup>2-</sup> ions there are 0.35 Mg<sup>2+</sup> ions and 0.65 Al<sup>3+</sup> ions in the 1 tetrahedral site, and 1.78 Al<sup>3+</sup> ions in the 2 octahedral sites. The other 0.22 octahedral sites are vacant. Let  $C_3$  denote the concentration of vacancies. Therefore  $C_3 = 1.6 \times 10^{21}$  cm<sup>-3</sup> for R-53, which is 6 times larger than  $C_3$  for the R-37 sample of Fe<sub>3</sub>O<sub>4</sub>. If neither the Mg and Al ions on the tetrahedral sites nor the Al ions and the vacancies on the octahedral sites are ordered, their random distribution will give rise to a mass fluctuation scattering. The  $\Gamma$  value for this random distribution of masses is calculated to be  $\Gamma = 4.4 \times 10^{-3}$ , 99% of this value is due to the vacancies. The phonon scattering caused by this

mass fluctuation can be calculated for low temperatures from Eq. (4). At 50°K this yields  $K_T = 2.4$  w/cm deg, and  $\theta\Lambda_0/T\Lambda_i^0 = 1.1 \times 10^7$ . At high temperature the theory of Ambegaokar<sup>90</sup> can be used. For  $T = \theta$  it will be assumed that the umklapp scattering leads to the same value of  $K_\theta$  as measured for MgAl<sub>2</sub>O<sub>4</sub>. Ambegaokar's theory applies for temperatures near  $T = \theta$ . The highest temperature at which comparison is possible from the available data in Figs. 4 and 5 is 500°K. Here the thermal resistivity value for MgAl<sub>2</sub>O<sub>4</sub> is 7.4 cm deg/w. The additional thermal resistivity that would be caused by the mass fluctuation scattering would be

$$\Delta W = 4\pi^2 V \theta \Gamma h^{-1} \bar{v}_g^{-2}, \quad (6)$$

where  $\bar{v}_g$  is  $7.0 \times 10^5$  cm/sec from Table IV. Using  $\Gamma = 4.4 \times 10^{-3}$  (which is  $\frac{1}{12}$  of that as defined by Ambegaokar),  $\Delta W$  is 4.3 cm deg/w. Thus the computed  $W$  for MgO·3.5Al<sub>2</sub>O<sub>3</sub> at 500°K is  $7.4 + 4.3 = 11.7$  cm deg/w, as compared to the observed value of 12.5 cm deg/w. Such agreement is considered satisfactory, especially since only the mass difference between the Al ions and the vacancies was considered in computing  $\Gamma$ . Any lattice distortion or changes in the elastic constants of the linkages<sup>62</sup> would serve to increase  $\Gamma$ . The lattice distortion around a metal ion vacancy, however, is probably small because the lattice structure is determined mainly by the fcc packing of the large radius O<sup>2-</sup> ions. The metal ion radius is about 40% that of the O<sup>2-</sup> ions, and they fit into the "interstices" in the oxygen lattice. Thus the mass difference may be the largest part of the vacancy effect.

The dashed curve labeled "boundary+vacancy" scattering in Fig. 5 was drawn for the combination of vacancy scattering calculated from Eqs. (4) and (6) and the boundary-plus-vacancy effect calculated by the method of Slack and Glassbrenner.<sup>67</sup> It is apparent that this calculated limiting curve for  $K$  of MgO·3.5Al<sub>2</sub>O<sub>3</sub> correctly predicts the general behavior, particularly from 50° to 500°K. Below 50°K the chemical impurities produce a  $K$  still lower than this limiting curve.

### Fe<sub>3</sub>O<sub>4</sub>

Now that the behavior of pure and impure MgAl<sub>2</sub>O<sub>4</sub> is understood in terms of the theory, it is possible to use the results for understanding Fe<sub>3</sub>O<sub>4</sub>. The experimental data for the Fe<sub>3</sub>O<sub>4</sub> runs R-37, R-57, and R-63 are shown in Figs. 6 and 7. The fact that Fe<sub>3</sub>O<sub>4</sub> has an orthorhombic crystal structure<sup>84</sup> at temperatures below  $T_x$  means that there are three principal thermal conductivities. Since the distortion from cubic is small, these three conductivities should be nearly equal. Therefore no effort was made to produce untwinned crystals,<sup>91</sup> and the results in Figs. 6 and 7 represent the average  $K$  for  $T < T_x$ . Figure 6 also contains the data of Kruckenberg<sup>1</sup> on natural Fe<sub>3</sub>O<sub>4</sub> crystals, Smit

<sup>88</sup> D. S. McClure, *Solid-State Physics*, edited by F. Seitz and D. Turnbull (Academic Press Inc., New York, 1959), Vol. 9, p. 399.

<sup>89</sup> W. Low and M. Weger, *Phys. Rev.* **118**, 1119 (1960).

<sup>90</sup> V. Ambegaokar, *Phys. Rev.* **114**, 488 (1959).

<sup>91</sup> W. C. Hamilton, *Phys. Rev.* **110**, 1050 (1958).

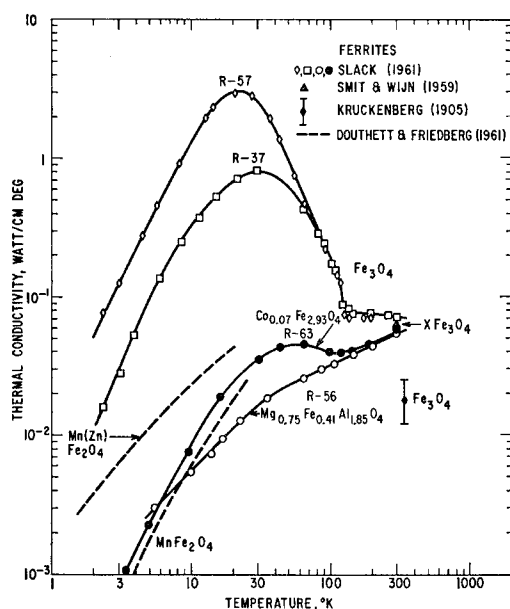


FIG. 6. The thermal conductivity vs temperature for various single-crystal ferrites. Data for a pleonaste spinel crystal, R-56, are shown for comparison.

and Wijn<sup>3</sup> on ceramic ferrite samples, and Douthett and Friedberg<sup>7</sup> on some single crystal ferrites. It is clear from the magnitude and temperature dependence of  $K$  in Fig. 6 that the explanation used for  $\text{MgO}$ ,  $\alpha\text{-Al}_2\text{O}_3$ , and  $\text{MgAl}_2\text{O}_4$  will have to be modified.

The most unusual feature for  $\text{Fe}_3\text{O}_4$  is the nearly temperature independent  $K$  found for the range  $119^\circ\text{K} \leq T \leq 300^\circ\text{K}$ . As mentioned previously,  $119^\circ\text{K}$  is the transition temperature  $T_x$  below which an ordering of the  $\text{Fe}^{2+}$  and  $\text{Fe}^{3+}$  ions on the octahedral sites takes place.<sup>25,26,91,92</sup> At this temperature the thermal conductivity exhibits an abrupt rise by a factor of 1.6. The details of this rise are shown more clearly in Fig. 7 where a linear plot of  $K$  vs  $T$  has been made. The transition temperature and its uncertainty from Fig. 7 is  $121 \pm 2^\circ\text{K}$ , which is essentially equal to the  $119.4 \pm 0.3^\circ\text{K}$  found by Calhoun<sup>25</sup> from electrical measurements on synthetic crystals. As the temperature decreases below  $119^\circ\text{K}$  the  $K$  rises, reaches a maximum, and then decreases, a behavior similar to that of the other diamagnetic crystals studied.

The thermal conductivity results for  $\text{Fe}_3\text{O}_4$  can be explained satisfactorily by assuming that phonons are the only important carriers of thermal energy. These phonons are assumed to be scattered by the standard processes found in the diamagnetic crystals, namely: other phonons (umklapp scattering), isotopes, vacancies, chemical impurities, and boundaries. One additional scattering mechanism then appears to be necessary. This is scattering of phonons from local disorder in the lattice formed by the magnetic moments of the

paramagnetic ions. This same model was found sufficient to explain the results for antiferromagnetic  $\text{MnF}_2$  and  $\text{CoF}_2$ .<sup>14</sup> Any possible magnon heat transport<sup>14</sup> appears to be unnoticeable in  $\text{Fe}_3\text{O}_4$ ,  $\text{MnF}_2$ ,  $\text{CoF}_2$ , or in  $\text{MnO}$ ,  $\text{CoO}$ , and  $\text{NiO}$ ,<sup>10,11</sup> using the present measuring techniques.

The electrical conductivity as a function of temperature was measured for several synthetic  $\text{Fe}_3\text{O}_4$  crystals very similar to R-37 and R-57. The results were almost the same as those reported by Calhoun.<sup>25</sup> The electrical conductivity is sufficiently low at all temperatures so that any electronic thermal conductivity contribution  $K_e$  is negligible. This lack of a significant  $K_e$  term is borne out by the agreement of the present data at  $300^\circ\text{K}$  with that of Smit and Wijn<sup>3</sup> on other ferrites. At room temperature these other ferrites have very low electrical conductivities<sup>3</sup> compared to  $\text{Fe}_3\text{O}_4$ .

The upper limits on the conductivity of  $\text{Fe}_3\text{O}_4$  imposed by umklapp and boundary scattering are shown in Fig. 8. The boundary limit for R-57 was calculated assuming diffuse reflection of phonons at the surface with  $d=0.24$  cm. The umklapp limit was drawn using the value of  $K_\theta=0.06$  w/cm deg estimated in the section under  $\text{MgAl}_2\text{O}_4$ . The value of  $\Gamma$  for pure, stoichiometric  $\text{Fe}_3\text{O}_4$  is so small that the  $K_I$  limit (see Table III) lies above the graph in Fig. 8. Therefore the results for the very nearly stoichiometric crystal, R-57, which has a vacancy concentration of about  $2 \times 10^{17} \text{ cm}^{-3}$  as computed in the section entitled Samples, do not approach the simple limits found for diamagnetic crystals for  $T < \theta$ . Only at temperatures near  $T=\theta$  where phonon-phonon scattering is dominant does the  $K$  for  $\text{Fe}_3\text{O}_4$  appear to approach that for diamagnetic crystals.

For  $T > 119^\circ\text{K}$  the  $\text{Fe}^{2+}$  and  $\text{Fe}^{3+}$  ions on the octahedral lattice sites are distributed randomly, and there is a rapid exchange of electrons from one  $\text{Fe}^{2+}$  to the

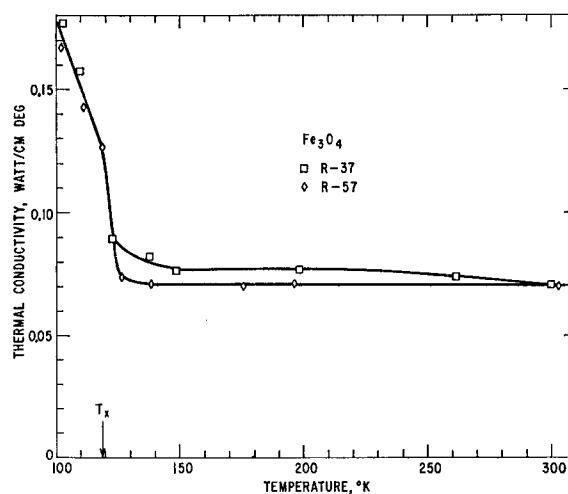


FIG. 7. The thermal conductivity vs temperature for synthetic  $\text{Fe}_3\text{O}_4$  crystals. There is a sharp rise in conductivity at  $121 \pm 2^\circ\text{K}$ , the temperature at which octahedral ordering of  $\text{Fe}^{2+}$  and  $\text{Fe}^{3+}$  occurs.

<sup>92</sup> R. Bauminger, S. G. Cohen, A. Marinov, S. Ofer, and E. Segal, Phys. Rev. **122**, 1447 (1961).

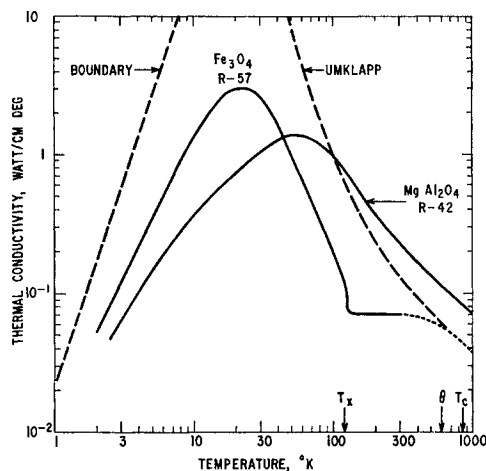


FIG. 8. A comparison of the thermal conductivity vs temperature for synthetic Fe<sub>3</sub>O<sub>4</sub> and natural MgAl<sub>2</sub>O<sub>4</sub> crystals. The dashed curves give the theoretical limits for Fe<sub>3</sub>O<sub>4</sub> imposed by boundary and umklapp scattering. The temperatures  $T_x$ ,  $\theta$ ,  $T_c$  are the transition, Debye, and Curie temperatures, respectively, of Fe<sub>3</sub>O<sub>4</sub>.

neighboring Fe<sup>3+</sup>. An incident compressible wave, a longitudinal phonon, can increase the overlap integrals, and, thus, may cause the octahedral ions to order. In this process of stress-induced ordering phonons will be absorbed, then these phonons will probably be reradiated incoherently, i.e., scattered. Such stress induced ordering has been observed before<sup>93</sup> for phonons of acoustical wavelengths in Fe<sub>3</sub>O<sub>4</sub>. This type of phonon scattering will occur as long as the octahedral ions are in the disordered state, i.e.,  $T > 119^\circ\text{K}$ . From the thermal conductivity results it appears that this scattering probability varies only slowly with temperature up to temperatures at least comparable with  $\theta$ . For  $T > \theta$  this scattering from the magnetic disorder may still be present, but it will be masked by umklapp scattering. The predominance of the umklapp scattering also means that any anomalous behavior in  $K$  on passing through the  $T_c$  at  $848^\circ\text{K}$  might also be effectively masked, even though further disorder in the magnetic arrangement is present above  $T_c$ .

An average value of the phonon mean free path  $l$  at  $T_x$  can be calculated from the simple Debye formula

$$K = \frac{1}{3} l \bar{v}_g C_v,$$

where  $C_v$  is the lattice specific heat per unit volume.  $C_v$  for the lattice can be estimated from the Debye function of  $\theta = 600^\circ\text{K}$ , and thus eliminate the magnetic specific heat contribution<sup>24</sup> near  $T_x$ . This computation yields an  $l_{gm}^0$  value<sup>14</sup> of  $60 \text{ \AA}$  for Fe<sub>3</sub>O<sub>4</sub> at  $T_x = 119^\circ\text{K}$ . This is to be compared with very similar values of  $l_{gm}^0$  found<sup>10,11</sup> in the antiferromagnetic oxides MnO and CoO, and with the much larger values of 4000 and

$2400 \text{ \AA}$  found<sup>14</sup> for the antiferromagnetic MnF<sub>2</sub> and CoF<sub>2</sub>.

As  $T$  decreases below  $119^\circ\text{K}$  the octahedral ions become progressively better ordered, but there does not appear to be a convenient measure of this order, such as the sublattice magnetization that was used to interpret the data on CoF<sub>2</sub>.<sup>14</sup> If an average mean free path  $l$  is computed from  $l = 3K\bar{v}_g^{-1}C_v^{-1}$ , then  $l$  versus  $T$  from  $60^\circ$  to  $115^\circ\text{K}$  can be fitted by

$$l = [4 \times 10^{-8} \text{ cm}] \exp(U/kT),$$

where  $U = 0.034 \text{ eV}$ . This value of  $U$  is about  $\frac{1}{3}$  of that found by Calhoun<sup>25</sup> from electrical resistivity measurements in this same temperature region. The exact significance of such an analysis of  $l$  is rather uncertain at present, and should be used with caution.

### Impure Fe<sub>3</sub>O<sub>4</sub>

The measurements on R-63 in which 2.4% of the Fe<sup>2+</sup> is replaced by Co<sup>2+</sup> ( $C_1 = 9.9 \times 10^{20} \text{ cm}^{-3}$  of Co) also show a break in the  $K$  curve near the  $T_x$  value for pure Fe<sub>3</sub>O<sub>4</sub>. The experimental value of  $T_x$  from Fig. 6 for this doped crystal is  $110 \pm 5^\circ\text{K}$ . The Co<sup>2+</sup> enters the spinel lattice on the octahedral sites<sup>18,94</sup> in place of Fe<sup>2+</sup>. Thus the octahedral ordering, which is responsible for the abrupt rise in  $K$  for crystals R-37 and R-57, has almost vanished in R-63. The randomly distributed Co<sup>2+</sup>, which has a magnetic moment different from that of Fe<sup>2+</sup>, cannot order at  $T_x$  because the temperature is too low for ionic diffusion to occur. The results on R-63 show that small concentrations of chemical impurities can have large effects on the  $K$  of Fe<sub>3</sub>O<sub>4</sub> at low temperatures by preventing ordering. The effect of small additions of Co may rapidly saturate because the  $K$  vs  $T$  curve for R-63 is very nearly the same as the one measured by Douthett and Friedberg<sup>7</sup> for a crystal approximating  $(\text{Zn}_{0.5}^{2+})(\text{Fe}_{0.5}^{3+})[(\text{Co}_{0.5}^{2+})(\text{Fe}_{1.5}^{3+})]\text{O}_4$ . Here, again, the Co<sup>2+</sup> is on the octahedral sites. The effect of such impurities at  $300^\circ\text{K}$  and above is small because the intrinsic disorder is already large.

The presence of other point imperfections, such as vacancies, can also affect the  $K$  of Fe<sub>3</sub>O<sub>4</sub>. This is clear from the comparison of the results for R-37 and R-57 in Fig. 6 for  $2^\circ\text{K} < T < 50^\circ\text{K}$ . Fe<sub>3</sub>O<sub>4</sub> crystal R-57 has a much lower vacancy concentration than R-37 and its thermal conductivity in this region is 4 times that of R-37. In R-37, the vacancy concentration  $C_3$  is  $2.6 \times 10^{20} \text{ cm}^{-3}$ , which is much larger than the known concentration of chemical impurities. The transition metals give  $C_1 = 1 \times 10^{18} \text{ cm}^{-3}$ , the other metals give  $C_2 = 3 \times 10^{18} \text{ cm}^{-3}$ . In crystal R-57 the calculated vacancy concentration is  $2 \times 10^{17} \text{ cm}^{-3}$ , which is much less than the concentration of chemical impurities. Therefore the vacancies are probably the dominant phonon scatterers in R-37 at  $10^\circ\text{K}$ , while for R-57 the chemical impurities

<sup>93</sup> W. P. Mason, *Physical Acoustics and the Properties of Solids*, (D. Van Nostrand Company, Inc., Princeton, New Jersey, 1958), p. 314.

<sup>94</sup> E. Prince, *Phys. Rev.* **102**, 674 (1956).

can introduce local disorder into the magnetic lattice, and thus cause phonon scattering.

A concentration of  $C_3 = 2.6 \times 10^{20} \text{ cm}^{-3}$  on the octahedral sites in R-37 will produce a mass fluctuation parameter of  $\Gamma = 6.6 \times 10^{-4}$ . Using the same arguments regarding vacancies at high temperatures ( $T \geq 30^\circ\text{K}$ ) that were used for the  $\text{MgO} \cdot 3.5\text{Al}_2\text{O}_3$ , the value of  $K$  calculated from this  $\Gamma$  using Eq. (4) is 2.5 w/cm deg at  $50^\circ\text{K}$ . The observed value is only  $\frac{1}{4}$  of this. Similarly the  $\Delta W$  computed from Eq. (6) is quite small. Therefore the fact that the vacancies in  $\text{Fe}_3\text{O}_4$  crystal R-37 have little effect on  $K$  for  $T > 50^\circ\text{K}$  is verified by the same theory that holds for diamagnetic crystals. The small difference (10%) between crystals R-37 and R-57 evident in Fig. 7 is probably not caused by vacancies but by experimental errors.

### Other Ferrites

Let us consider the  $K$  measurements on the other single crystal ferrites. The  $K$  vs  $T$  curves for some poorly defined ferrites measured by Douthett and Friedberg<sup>7</sup> are shown in Fig. 6. Their  $K$  vs  $T$  curve for  $\text{Co}(\text{Zn})\text{Fe}_2\text{O}_4$  is nearly the same as that for the  $\text{MnFe}_2\text{O}_4$  curve, and is not shown. Their measurements on these Linde<sup>22</sup> ferrite samples extend from  $1.5^\circ$  to  $25^\circ\text{K}$ , but the  $K$  vs  $T$  curves could reasonably be extrapolated to the point in Fig. 6 marked  $\text{XFe}_2\text{O}_4$ . Smit and Wijn<sup>3</sup> state that the  $K$  value given for  $\text{XFe}_2\text{O}_4$  (where  $X$  is some metallic ion) is reasonably representative of all spinel ferrites at  $300^\circ\text{K}$ . From the results on R-63 it appears reasonable to conclude that the ferrite curves of Douthett and Friedberg would not exhibit any pronounced rise in  $K$ , such as found in  $\text{Fe}_3\text{O}_4$ . In fact,  $K$  may decrease monotonically as  $T$  decreases below  $300^\circ\text{K}$ . This is quite similar to the behavior for  $\text{Mg}_x\text{Fe}_{1-x}\text{Al}_2\text{O}_4$ , also shown again in Fig. 6. Some measurements of  $K$  for nickel ferrite,  $\text{Ni}(\text{Fe})\text{Fe}_2\text{O}_4$ , made by White and Woods<sup>95</sup> gave results similar to those in Fig. 6 for  $\text{Mn}(\text{Zn})\text{Fe}_2\text{O}_4$ .

It is known that all of these ferrites,  $\text{MnFe}_2\text{O}_4$ ,  $\text{Mn}(\text{Zn})\text{Fe}_2\text{O}_4$ ,  $\text{Co}(\text{Zn})\text{Fe}_2\text{O}_4$ , and  $\text{Ni}(\text{Fe})\text{Fe}_2\text{O}_4$ , are either partially random spinels or inverse spinels. None are normal spinels. For instance  $\text{MnFe}_2\text{O}_4$  has the distribution<sup>96</sup>  $(\text{Mn}_{0.8}^{2+})(\text{Fe}_{0.2}^{3+})[(\text{Mn}_{0.2}^{3+})(\text{Fe}_{0.1}^{2+})-(\text{Fe}_{1.7}^{3+})]\text{O}_4$ . Here the unbracketed group is distributed randomly over the tetrahedral sites, and the  $[\ ]$  group randomly over the octahedral sites. This is similar to the  $\text{Co}_{0.07}\text{Fe}_{2.93}\text{O}_4$  in that the random distribution is frozen in during cooling, and the magnetic lattices exhibit many local fluctuations. It appears that phonons are quite effectively scattered by such a disordered magnetic lattice at low temperatures.

Douthett and Friedberg<sup>7</sup> observed an increase in

the  $K$  of the  $\text{MnFe}_2\text{O}_4$  and  $\text{Co}(\text{Zn})\text{Fe}_2\text{O}_4$  in an applied magnetic field of 9400 oe. A preliminary search for a change in  $K$  with applied magnetic fields up to 5700 oe was made at  $110^\circ\text{K}$  in an  $\text{Fe}_3\text{O}_4$  crystal similar to R-37. No noticeable effect, i.e. a change in  $K$  of  $>5\%$ , was found. No further checks either at  $4^\circ\text{K}$  or at  $300^\circ\text{K}$  have yet been made.

The general picture of phonon scattering by disordered magnetic lattices, but not by ordered ones, indicates that thermal conductivity measurements on several different crystals might exhibit unusual behavior. For instance,  $\text{ZnFe}_2\text{O}_4$  is a normal spinel<sup>97</sup> and becomes antiferromagnetic<sup>98</sup> below  $9.5^\circ\text{K}$ . Above  $9.5^\circ\text{K}$  it is paramagnetic. Thus an abrupt rise in the thermal conductivity of  $\text{ZnFe}_2\text{O}_4$  might be seen at  $9.5^\circ\text{K}$ . A similar anomaly at low temperatures might appear in  $\text{CdFe}_2\text{O}_4$ , which is a normal spinel<sup>99</sup> and is quite similar to  $\text{ZnFe}_2\text{O}_4$ .

### Point Impurity Effects for $T < 30^\circ\text{K}$

For none of the crystals studied in the present experiment was the  $K$  in the temperature range  $T < 30^\circ\text{K}$  as high as the limit imposed by boundary scattering alone. Crystal R-38 of  $\text{MgO}$  came the nearest to this limit, but even its  $K$  was a factor of 2 low. The excess thermal resistivity is attributed to chemical impurities. Three different kinds of impurities have been mentioned: transition metals with a concentration  $C_1$ , non-transition metals with a concentration  $C_2$ , and vacancies with a concentration  $C_3$ . In order to establish a general type of behavior the thermal resistivity at  $10^\circ\text{K}$ ,  $W(10^\circ\text{K})$ , has been plotted as a function of concentration for all 10 crystals in Fig. 9. Where available, all three concentration values  $C_1$ ,  $C_2$ , and  $C_3$  have been entered. If the  $\text{MgO}$  and  $\text{MgAl}_2\text{O}_4$  crystals, 7 in number, are considered, then the best correlation of  $W(10^\circ\text{K})$  versus concentration is obtained by considering only  $C_1$  and drawing the broad diagonal line shown in Fig. 9. This line indicates a relationship of the form  $W(10^\circ\text{K}) \sim C_1^n$ , when  $n = +0.8$ . An exact correlation is not expected since the  $C_1$  values are only accurate to within a factor of 2, and since it is not really expected that all transition metal impurities will behave in the same way. The correlation of  $W(10^\circ\text{K})$  with  $C_2$  (or  $C_3$ ) is considerably worse than that with  $C_1$ . The  $W(10^\circ\text{K})$  versus  $C_1$  values for  $\text{Fe}^{2+}$  doped  $\text{ZnSO}_4 \cdot 7\text{H}_2\text{O}$  of Rosenberg and Sujak,<sup>69</sup> for  $\text{Mn}^{2+}$  doped  $\text{NaCl}$  of Klein,<sup>71</sup> and for  $\text{Cr}^{3+}$  doped  $\alpha\text{-Al}_2\text{O}_3$  of Berman, Foster, and Rosenberg<sup>100</sup> have also been entered in Fig. 9. The data for  $\text{ZnSO}_4 \cdot 7\text{H}_2\text{O}$  and  $\text{NaCl}$  fall on the line to

<sup>97</sup> J. M. Hastings and L. M. Corliss, *Revs. Modern Phys.* **25**, 114 (1953).

<sup>98</sup> J. M. Hastings and L. M. Corliss, *Phys. Rev.* **102**, 1460 (1956); E. F. Westrum and D. M. Grimes, *J. Phys. Chem. Solids* **3**, 44 (1957).

<sup>99</sup> E. J. W. Verwey and E. L. Heilmann, *J. Chem. Phys.* **15**, 174 (1947).

<sup>100</sup> R. Berman, E. L. Foster, and H. M. Rosenberg, *Defects in Crystalline Solids* (The Physical Society, London, 1955), p. 321.

<sup>95</sup> G. K. White and S. B. Woods, as reported in reference 7 footnote, p. 1665.

<sup>96</sup> F. W. Harrison, W. P. Osmond, and R. W. Teale, *Phys. Rev.* **106**, 865 (1957).

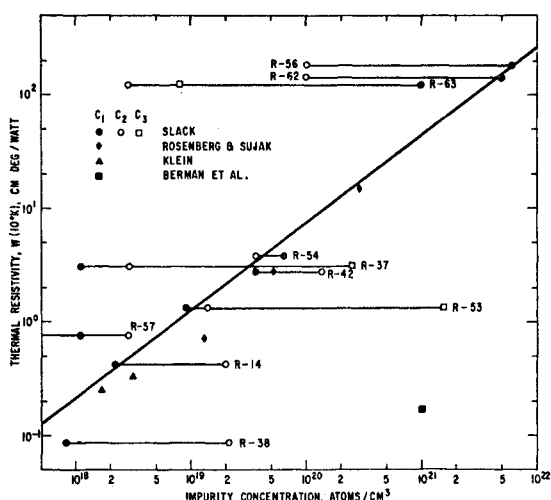
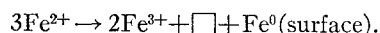


FIG. 9. A composite graph of the measured thermal resistivity at 10°K,  $W(10^\circ\text{K})$ , as a function of impurity concentration. The values  $C_1$ ,  $C_2$ ,  $C_3$  are explained in the text. The diagonal line is the "best-fit" if  $W(10^\circ\text{K})$  depends mainly on  $C_1$ , the transition metal concentration.

within a factor of 2 in spite of the very different crystal structures and impurity environments. However, the data of Berman *et al.*<sup>100</sup> on  $\alpha\text{-Al}_2\text{O}_3$  disagree by a factor of at least 100, thus indicating that the phonon scattering in this temperature region does depend on the particular nature of the transition metal impurity. Orbach's<sup>87</sup> analysis of  $\text{Fe}^{2+}$  in  $\text{ZnSO}_4 \cdot 7\text{H}_2\text{O}$  describes one such particular scattering process. In this process it appears from Fig. 9 that  $n$  in  $C_1^n$  is nearly  $n=1.0$ . In the theory of phonon-spin interaction given by Orbach,<sup>87</sup>  $W$  cannot be simply proportional to  $C^n$ . A more complex dependence involving temperature, scattering cross-section, and concentration is expected. Figure 9 simply indicates that  $W$  increases monotonically with  $C$ , and that some transition metals have roughly similar effects in various host crystals.

The results on  $\text{Fe}_3\text{O}_4$  (crystals R-37, R-57, R-63) tend to fit the same general pattern as MgO and  $\text{MgAl}_2\text{O}_4$ . The main difference is that both diamagnetic and paramagnetic impurities can produce disorder in the magnetic lattice of  $\text{Fe}_3\text{O}_4$  by substituting for an Fe atom. Whether diamagnetic impurities such as Al and Na have as large an effect as the paramagnetic Co cannot be decided from Fig. 9. However it is clear from Fig. 9 that Fe vacancies (see R-37) have a scattering cross-section at 10°K only 2 to 10% of that of the chemical impurities. A vacancy  $\square$  is produced in the cation lattice according to



The change in the spin only magnetic moment in the interior of the crystal is

$$\Delta S = 2(5/2) - 3(4/2) = 1,$$

or an average  $\langle \Delta S \rangle_{av}$  per lattice site of  $\frac{1}{3}$ . When an

$\text{Fe}^{3+}$  ion is replaced by  $\text{Al}^{3+}$ , then  $\langle \Delta S \rangle_{av} = \frac{5}{2}$ . It seems plausible to assume that the scattering cross section of a defect increases with  $\langle \Delta S \rangle_{av}$ . Hence an Al atom should have a greater effect than a vacancy. This argument indicates why vacancies may be much less effective scatterers than substitutional diamagnetic impurities in  $\text{Fe}_3\text{O}_4$ .

In order to reach the boundary scattering limit in  $\text{Fe}_3\text{O}_4$  at 10°K for  $d=0.24$  cm the vacancy concentration should be less than  $\sim 10^{18} \text{ cm}^{-3}$  and the chemical impurity content less than  $\sim 10^{17} \text{ cm}^{-3}$ . Rather special efforts would be required in order to obtain such pure  $\text{Fe}_3\text{O}_4$ .

### CONCLUSIONS

The thermal conductivity of single crystals of MgO,  $\text{MgAl}_2\text{O}_4$ ,  $\text{MgO} \cdot 3.5\text{Al}_2\text{O}_3$ ,  $\text{Mg}_x\text{Fe}_y\text{Al}_z\text{O}_4$ , and  $\text{Fe}_3\text{O}_4$  has been measured from 3° to 300°K.

The present results for MgO and previous ones for  $\alpha\text{-Al}_2\text{O}_3$  are explicable in terms of the theory of phonon scattering by umklapp processes, by isotopes, and by crystal boundaries. The thermal conductivity of pure crystals of the double oxide  $\text{MgAl}_2\text{O}_4$  can be considered to be approximately an average between the results for MgO and  $\alpha\text{-Al}_2\text{O}_3$ . The thermal conductivity of the natural crystals studied is, however, considerably reduced at low temperatures by the presence of chemical impurities, particularly transition metal impurities.

The study of  $\text{MgO} \cdot 3.5\text{Al}_2\text{O}_3$  and  $\text{Mg}_x\text{Fe}_y\text{Al}_z\text{O}_4$  indicates that the thermal conductivity of  $\text{MgAl}_2\text{O}_4$  can be somewhat reduced by the presence of vacancies, and greatly reduced by the presence of large quantities of Fe.

The measurements on  $\text{Fe}_3\text{O}_4$  indicate that phonons are the dominant carriers of thermal energy, and that any magnon or electron heat transport is very small. In addition to the scattering mechanisms found in the diamagnetic crystals, the phonons in  $\text{Fe}_3\text{O}_4$  and other ferrites can be scattered by local disorder in the magnetic lattice. Vacancies as well as chemical impurities can produce such local disorder, but vacancies are much less effective than the impurities.

### ACKNOWLEDGMENTS

The author wishes to thank R. L. Hansler for the synthetic MgO crystals and F. H. Horn for the synthetic  $\text{Fe}_3\text{O}_4$  crystals. Special thanks are due J. H. McTaggart for his help in sample preparation and for many of the thermal conductivity measurements. The electrical resistivity measurements on the  $\text{Fe}_3\text{O}_4$  were made by P. P. Friguetto and W. E. Engeler, and the magnetic field effect on the thermal conductivity of  $\text{Fe}_3\text{O}_4$  was performed by R. M. Chrenko. The aid of D. E. Jenson of Ward's Natural Science Establishment, Incorporated, in obtaining the natural  $\text{MgAl}_2\text{O}_4$  and  $\text{Mg}_x\text{Fe}_y\text{Al}_z\text{O}_4$  crystals is also much appreciated. Various conversations with R. Orbach have been helpful in understanding paramagnetic impurities.